火山 第58巻（2013）
第2号，CD-BOOK

2013 IAVCEI Field Trip Guide

B01: Active Volcanoes in Northeast Japan

Masao Ban*, Tsukasa Ohba**, and Akihiko Fujinawa***

**: Department of Earth and Environmental Sciences, Faculty of Science, Yamagata University, Japan*
***: Faculty of Engineering and Resource Science Akita University, Japan*
****: Earth Environmental Science Course, Faculty of Science, Ibaraki University, Japan*

1. Introduction

Northeast Japan, a mature island arc, has many stratovolcanoes along with some other volcano types. Eighteen of these volcanoes are active. Most of the stratovolcanoes in northeast Japan are thought to follow a general evolutional course consisting of (1) cone building, (2) caldera collapse, and (3) post-caldera stages. Among the 18 active volcanoes in northeast Japan, we will visit the following six active volcanoes and observe the geologic features of their activities during various evolutional stages: the Iwate volcano, which is in the cone-building stage; the Bandai volcano, which is in the caldera-forming stage; and the Azuma, Zao, Akita-Yakeyama, and Hachimantai volcanoes, which are in the post-caldera stage. The latest eruptions took place in AD 1888 at Bandai, in AD 1977 at Azuma, in AD 1940 at Zao, in AD 1919 at Iwate, and in AD 1997 at Akita-Yakeyama. Among these, the 1888 eruption in Bandai is famous for a sector collapse that accompanied a debris avalanche phenomenon, which was the first ever reported in the world. Around Akita-Yakeyama, one can enjoy a spectacular view of a geothermal field. We will also visit Ichinomegata maar (80 to 60 ka), which features mantle xenoliths, and the Toga tuff ring. In the first half of this article, we will explain geological and petrological features of each volcano where we will visit as well as tectonic and volcanological background of northeast Japan, and in the second half we will explain the details of the observation points in each volcano.

1-1. Tectonic setting of northeast Japan

In northeast Japan, the volcanic front is situated ca. 100 km above the seismic plane of the Pacific Plate, which is subducting at an angle of about 30 degrees westward beneath the North American Plate. The volume distribution of volcanic materials, excluding caldera-related felsic rocks, clearly reveals the existence of two volcanic chains: the frontal row (Nasu volcanic zone) and the back arc row (Chokai volcanic zone) (*e.g.*, Kawano *et al.*, 1961; Tatsumi and Eggins, 1995). These chains are also geochemically distinct, as may be seen in the lower K_2O content in the frontal row (*e.g.*, Kawano *et al.*, 1961). These features are observed in many subduction zones (Tatsumi and Eggins, 1995). The locations of the six active volcanoes where we will visit are shown in Fig. 1.

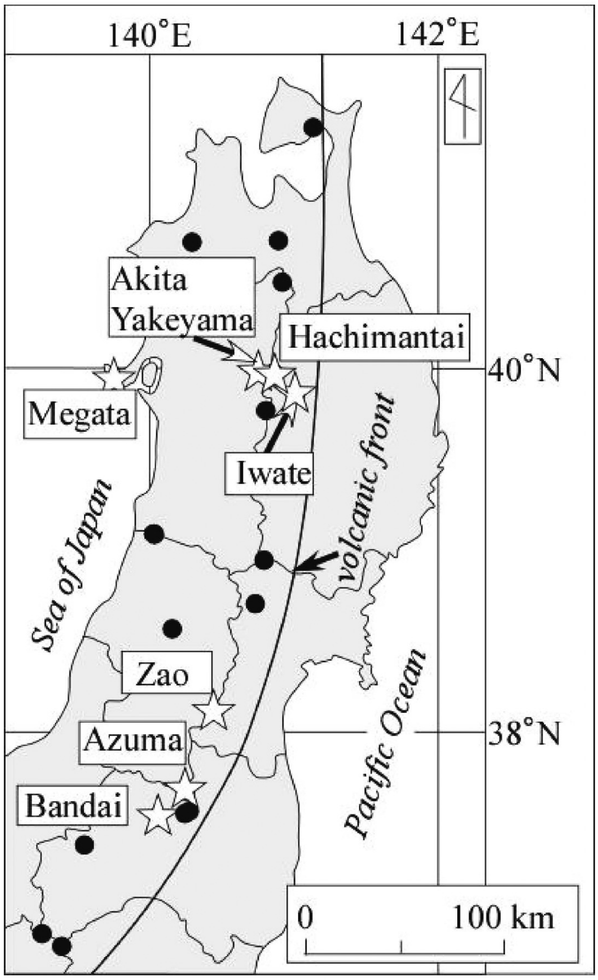

Figure 1. Locality map of the active volcanoes in northeast Japan (closed circle and star). We will visit the volcanoes with the star symbol.

Another important feature of the spacing of volcanoes in northeast Japan is the cluster

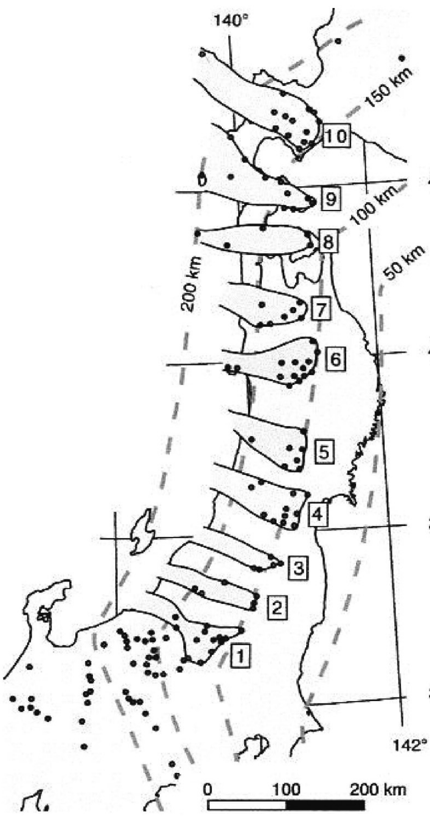

Figure 2. Distribution of volcanoes younger than ca. 1 Ma in northeast Japan, after Tamura *et al.* (2002).

distribution of frontal volcanoes (Fig. 2) (Umeda *et al.*, 1999; Tamura *et al.*, 2002). One cluster is composed of ~10 volcanoes and is 10 to 30 km in size. The intervals of the clusters are 70～100 km. Further, rear arc side volcanoes distribute only behind the clusters. Tamura *et al.* (2002) interpreted this finger-like spatial distribution as corresponding to that of the hot area (hot fingers) of the mantle wedge. These predicted hot fingers have been confirmed by the examination of seismic tomography (*e.g.*, Nakajima *et al.*, 2001; Wang and Zhao, 2005; Huang *et al.*, 2011).

1-2. Across-arc variation in petrologic feature relating to the down going slab

In northeast Japan, the systematic across-arc variation in the chemical compositions of Quaternary basalts, such as the increase of K_2O and incompatible trace elements from the front to the back arc side, has been recognized (*e.g.*, Kuno, 1966; Kawano *et al.*, 1961; Sakuyama and Nesbitt, 1986; Nakagawa *et al.*, 1988). This zonal variation correlates with the depth of the down-going slab and has been explained by the combined processes of different degrees of partial melting of the mantle wedge and difference in dehydration phases both in the down-going slab and the down-dragged hydrous layer at the base of the mantle wedge (*e.g.*, Tatsumi *et al.*, 1983; Tatsumi and Eggins, 1995).

Kimura and Yoshida (2006) analyzed Pb-Nd-Sr isotopic ratios as well as major and trace elements on systematically sampled basaltic rocks from Quaternary volcanoes in northeast Japan.

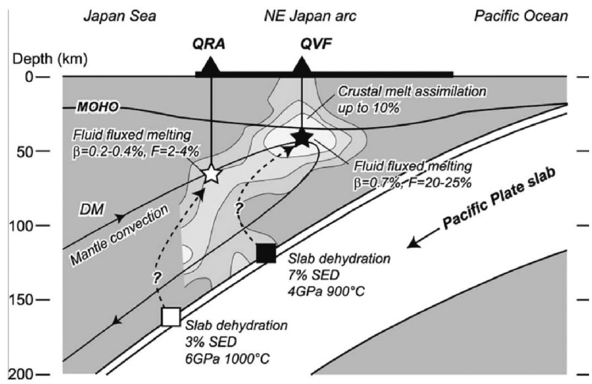

Figure 3. Schematic representation of the generation of primary magmas in the northeast Japan arc, after Kimura and Yoshida (2006).

They examined degrees of contributions of source mantle, subduction components, and crustal components to the least differentiated basaltic magmas, as well as the degrees of melting of source materials in producing the primary magmas. Figure 3 presents the results. They found a larger percentage of contribution of lower crustal materials than ever reported.

Tatsumi *et al.* (2008) examined the genetic relationship between calc-alkaline and tholeiitic magmas coexisting in the Zao volcano, by a full petrologic data set including the micro-analyses of isotopic and trace element compositions of phenocrysts. One of important results is that the primary magma of calc-alkaline series was formed by the melting of the upper mantle, while that of tholeiitic series was by the lower crust. This result is totally opposite to that of many previous studies. Takahashi *et al.* (2012) performed the same study on Azuma volcano and obtained similar results as Tatsumi *et al.* (2008).

2. Bandai volcano

2-1. Introduction

The Bandai volcano is one of the active volcanoes in the northeast Japan arc. The volcano is located about 20 km west of the volcanic front. The volcano is a conical stratocone, 7 to 10 km in diameter and about 1 km in relative height. The stratocone consists of four spatially overlapped composite volcanic edifices: the Akahaniyama,

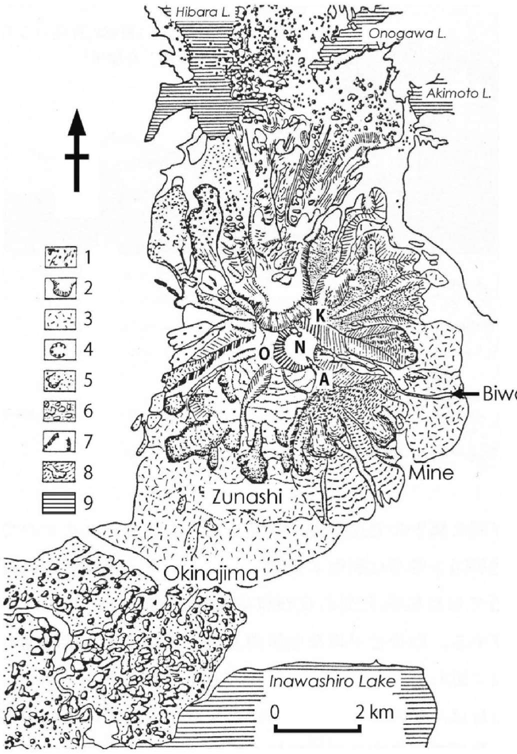

Figure 4. Geomorphological map of the Bandai volcano (modified from Fig. 1 of Moriya, 1988): 1, 1888 debris avalanche surface; 2, amphitheater of 1888 eruption; 3, fan deposits; 4, Numanodaira crater; 5, slopes of the Ohbandai volcano; 6, Okinajima avalanche surface; 7, southwest facing amphitheater; 8, slopes of main stratovolcanoes; 9, lakes.

Kushigamine, Oh-Bandaisan, and Ko-Bandaisan edifices, with a summit explosion crater that is surrounded by the peaks of the four edifices, opening toward the east (old Numanodaira crater) (Fig. 4). There were several crater lakes and sulfuric fumaroles near the old Numanotaira crater before the 1888 explosion event. Moreover, at the northwest side of the summit several local hot springs were utilized. The phreatic explosion on 15th July 1888 gave rise to the most conspicuous amphitheater in the Bandai volcano of ca. 2.5 km in diameter opening to the north.

2-2. Geology

The basement rocks of the Bandai volcano consist of the granodioritic plutonic rocks of Cretaceous age, and its overlying conglomerate, sandstone, siltstone, and andesitic to rhyolitic lavas and pyroclastics of Miocene age. Welded tuff of the lower Pleistocene age is also cropped out in the southwestern foot of the volcano.

2-2-1. Volcanic edifices

The eruption and formation of the Bandai volcanic edifice might have been initiated more than 0.7 Ma. Precursory volcanisms represented by formation of lava domes and block and ash flow deposits in the north area occurred ca. 0.5 Ma. The development history of the main edifice consists of four independent formation stages of the Akahaniyama, Kushigamine, Oh-Bandaisan, and Ko-Bandaisan edifices in descending order, with several intercalating sector collapse events between the stages (Fig. 5). The former two edifices were formed during 0.4 to 0.1 Ma, whereas the latter two were developed later than 0.08 Ma (Fig. 6).

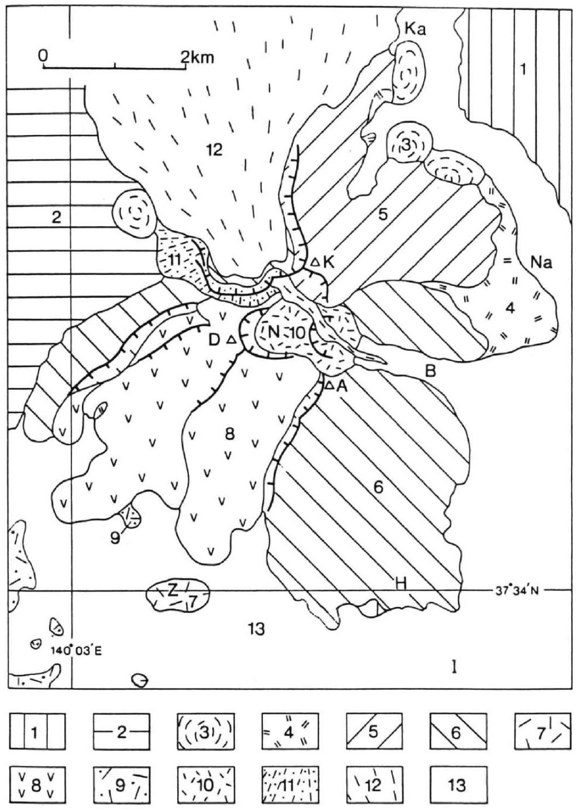

Figure 5. Geologic summary map of the Bandai volcano, after Mimura and Nakamura (1997), partly modified.

The Akahaniyama edifice is the oldest stratocone, which had been built up ca. 0.4 Ma and covered a similar basal size to the present Bandai volcano. The edifice has been altered, weathered, and eroded, with only a strongly dissected, thin pyramidal body remaining in the east to the southeastern part of the volcano. The main stratocone is made up of more than three lava flows

Geologic Time	Stratigraphic Dvision		Age (Ma)	Tephra along Foothills
Holocene	New Bandai Volcano	Debris Avalanche Deposits of 1888 and 1954		Kuroboku Soil
		Biwazawa Debris Avalanche Deposit	0.005	
		Kobandai Volcanic Cone		
		Numarotaira Debris Avalanche Deposit		Hayama Loam Formation
Pleistocene		Ohbandai Volcanic Cone/Zunashi Debris Avalanche Deposit	0.07	
		Okinajima Debris Avalanche Deposit/Pumice Layers	0.09	
	Old Bandai Volcano	Kushigamine Volcanic Cone/Akahani Volcanic Cone	0.1	Mineyama Loam Formation
		Nagasaka Pyroclastic Flow Deposits		
		Kawakami Lava Dome Cluster	0.5	
	Pre-Bandai Volcano	lava of the base of the 1888 avalanche scarp	0.7	

Figure 6. Summary of stratigraphy of the Bandai volcano, after Mimura and Nakamura (1997).

with their intercalating ash-fall layers, and agglutinate layer more than 30 m thick at its summit. Many lava lobes are also recognized near the foot of the edifice.

Kushigamine is the secondly developed stratocone in the eruption history of the Bandai volcano, and the edifice overrides the northern part of the Akahaniyama cone. The Kushigamine cone is composed of more than four units of lava flows. The lower two units are about 150 m thick, and the strata are of aphyric andesitic or obsidian-like massive lavas with an intercalating air-fall ash layer. The base of the cone is ca. 1.5 km in radius. Upper units flowed northeastward to make up the fringe of lava lobes near its foot.

Oh-Bandaisan is a conical edifice with its peak at the present summit of the Bandai volcano. Oh-Bandaisan was built up in the amphitheater due to the collapse of the Akahaniyama cone. Repeated Strombolian eruptions deposited air-fall tephra more than 300 m thick to make up the central pyroclastic cone that is 1.5 km in diameter. Several lavas flowed southward in the later stage of the Oh-Bandaisan development, to build up clear lava toes up to 120 m thick. Although the lava flows in this stage commonly show evident toes, their microstructures on the surfaces, such as lava wrinkles and lava levee, are obscured, probably due to the mantling of recent tephra.

Ko-Bandaisan is the conical stratocone that suddenly collapsed during the 1888 explosion. The wreck of the cone is scarcely observed at and outside of the AD 1888 amphitheater. A roughly stratified tephra deposit of more than 100 m thick is cropped out on the wall of the amphitheater. It consists of an alternation of volcanic blocks with maximum diameter exceeding 2 m and volcanic sands. Several feeder dikes are also observable in the tephra deposit.

2-2-2. Sector collapses and debris avalanche deposits

The Bandai volcano experienced at least four sector collapse events during its development history, and caused huge amounts of debris avalanche deposits in the both the northern and the southern feet of the volcanic edifices. The latest collapse will be described in the next section (section 2-3. Historic eruptions).

Sector collapse of Akahaniyama and Okinajima debris avalanche

The collapse of the Akahaniyama cone gave rise to the Okinajima debris avalanche deposit, which covers an area of 50 km^2 extending from the southern foot of the volcano westward to the Kitagata city of the Aizu basin via the old Nippashi river. The southward branch of the deposit dammed up the river, which might have given rise to the lake Inawashiro. The avalanche deposit consists mainly of fragile pyroclastics of the Akahaniyama origin, with more than 30 m in thickness. Enormous hummocky hills of 100 to 400 m in base diameter with relative heights of 1 to 50 m are still observable on the surface of the Okinajima debris avalanche deposit. The farthest hummocky hill is recognized at 25 km southwest of the present summit. The total amount of the deposit is estimated at about 4 km^3 (Yamamoto and Sudo, 1996). The oldest amphitheater in the Akahaniyama area has been almost completely buried up by the ejecta of the later stages, during the development of Oh-Bandaisan and Ko-Bandaisan.

The direct trigger of the collapse may have been the intrusion of silicic magma that erupted as a gigantic fallout pumice immediately after the collapse of Akahaniyama. The ^{14}C age of the organic carbon in the pumice fall deposit indicates that the collapse and its related explosive eruption occurred at about 46 ka (Yamamoto *et al.*, 2005).

Collapse of Oh-Bandaisan and Suriagehara fan and lahar deposit

The Suriagehara fan and lahar deposit drapes the surface of the Okinajima debris avalanche deposit in the southwestern foot of the volcano around the Zunashi and Suriagehara areas. This deposit is composed of debris avalanche and lahar layers with intercalating thin sand and silt beds (Yamamoto and Sudo, 1996). Judging from their lithology and lithofacies, this must have resulted from some kind of landslide or collapse. The ^{14}C age of wood chips in the deposit is about 14 ka (Yamamoto and Sudo, 1996).

Numanodaira, Biwazawa collapse

After the formation of the Oh-Bandaisan edifice was completed, a collapse occurred near the summit, to cause a horseshoe-shaped crater 700 m wide and opening eastward. A debris avalanche deposit with distinct hummocky hills on its surface emplaced on the floor of the Numanodaira. The debris avalanche deposit further collapsed to form another horseshoe-shaped failure wall at the top of the Biwazawa valley. A fan deposit probably due to this collapse also developed along the Biwazawa valley near the foothill of the edifice. We can find a small hummocky hill near the margin of the fan deposit.

2-3. Historic eruptions

2-3-1. AD 1888 eruption

Sequence of the AD 1888 eruption

The reliable historic eruption of the Bandai volcano happened only once. It occurred almost suddenly, on the morning of 15th July 1888, with no conspicuous precursory phenomena.

The sequence of the Bandai AD 1888 eruption was summarized by Fujinawa *et al.* (2008) as follows.

Table 1. Sequence of the Bandai AD 1888 eruption, after after Fujinawa *et al.* (2008) partly revised.

year, month day	time	phenomena
1888, July		
8th to 14th		Slight quakes and rumbling were recognized near the edifice
15th	7:00	Weak earthquake
	7:30	Strong earthquake
	7:45	A violent earthquake triggered the explosion. Some of the 15-20 explosions caused pyroclastic surge(s), the edifice was fully covered by black smoke.
	7:46	Collapse of the edifice induced a debris avalanche .Pyroclastic surge accompanying ash cloud reached the eastern foot of the volcano.
	7:55	Debris avalanche ceased. Phreatic explosions were recognized for several times.
	8:05-9:00	Other pyroclastic surge(s) flowed down the eastern side of the volcano. Eruption column gradually formed an umbrella part. Warm rain fell. Rain fall-derived lahar originated in the deposition area. Ash cloud cleared away around the edifice.
	16:00	Ash fall ceased in the distal part.

Information related to the Bandai AD 1888 eruption event (Table 1) was collected from Sekiya and Kikuchi (1890) and the Centennial Project Body of the Bandai Eruption (1988). Small earthquakes were felt for a week before the catastrophic explosion. On the morning of 15th July, earthquakes occurred continually, beginning at 07:00. Explosions commenced at around 07:45, with the volcano ejecting accessory blocks, lapilli, and ash with one burst after another up to 20 times a minute; the final one triggering the collapse of the edifice and causing a debris avalanche. The eruption column reached almost the same height as the relative height of the summit (ca. 1200 to 1300 m) above the crater rim (Sekiya and Kikuchi, 1890). The first and biggest pyroclastic surge must have occurred during the barrage of explosions (Yamamoto *et al.*, 1999). The eruption column continued ascending afterward and finally reached a height of 5000 m above the summit, where an umbrella shape developed (Nakamura and Aoki, 1980). A couple of pyroclastic surge events might have followed the first surge. A Buddhist priest (Tsurumaki Johgen) who was staying at the

"Nakanoyu" spa on the western side of the edifice, recorded that "the second and third bursts successively occurred several tens of minutes after the first burst". Another witness, Mr. Kinshiro Ichinose, supported this sequence of events. He noted that "about 20 min after the arrival of the first black smoke, the second black smoke arrived" (cited in Yamada, 1988). Hot water rained at the eastern foot of the edifice around 10:00, and the eruption ceased soon afterwards. Another testimony, which is of help in revealing the flow conditions of the surge, appeared in the Centennial Project Body of the Bandai Eruption (1988). An eyewitness, Mr. Mutoh, said, "It was fully clear in the morning of 15 July, but suddenly there was rumbling in the north and an earthquake abruptly occurred immediately after that. Quakes and tremors successively occurred for 10 min, with subsequent formation of an eruption column of about '30 m high' (might be his misunderstanding) discharging from the summit area. Therefore, I ran about 300 m toward my home, but I was caught by black smoke accompanying strong wind, which prevented me from going back home. I had no choice but to go another direction, so I ran eastward about 200 m.

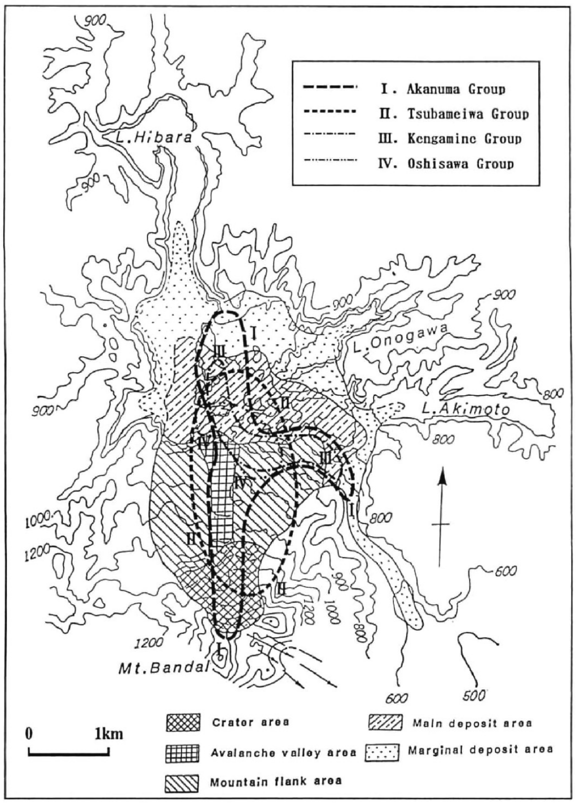

Figure 7. Distribution map of AD 1888 debris avalanche deposits, after Nakamura and Glicken (1997), partly modified.

Abruptly, a violent blast blew me unconscious about 25 m, to the foot of the wall (fence), so that I crouched at the western end of the wall. Soon after that, the black cloud came up to me with a frightening sound just like dong-dong, warrie-wari. Terribly hot ash fell from the black smoke over the southern slope to the foot of the volcanic edifice."

Topographic change

Immediately after the eruption, the newly formed amphitheater was 2466 m wide (EW) and 220 m long (NS), opening to the north. The crater wall was 4 km long, and the maximum relative height of the wall was up to 400 m. The volume of the collapsed edifice was approximated as 1.2 km^3 (Sekiya and Kikuchi, 1888). The debris flowed northward and the avalanche deposit covered an area of 35 km^2, with the total volume as much as 1.5 km^3. The deposit dammed up three streams to produce the Hibara, Onogawa, and Akimoto lakes,

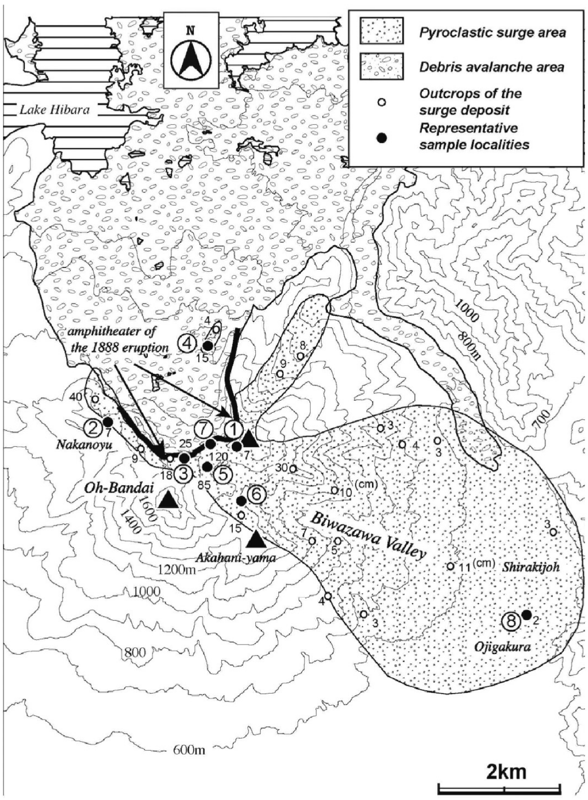

Figure 8. Distribution of pyroclastic surge and debris avalanche, after Fujinawa *et al.* (2008).

resting many hummocky hills on its surface. A box canyon called avalanche valley, 600 m wide and 3 km long, was also formed between the crater area and the main deposition area (Fig. 7).

Air fall ash

The air fall ash deposit of the AD 1888

eruption extended eastward from the crater, depositing 30 to 20 cm thick at the eastern foot of the edifice (Shirakijoh and Okenokuchi), and reached to the coastal region of the Pacific Ocean.

Surge deposit

It has been suggested that the "blast" (Nakamura and Glicken, 1988) or "pyroclastic density current" (Yamamoto *et al.*, 1999) generated, along with the debris avalanche and fallout ash from the eruption column, what we call here the pyroclastic surge. The surge deposits can be observed in the summit area surrounding the amphitheater and in the eastern to southeastern flanks along the Biwazawa ravine, reaching as far as 7 km from the rim of the amphitheater (Fig. 8). The deposits on the amphitheater floor are mostly covered by epiclastic volcaniclastic deposits, but can be observed at several sites (*e.g.*, loc. 4 in Fig. 8). The deposit of the 1888 eruption ejecta tends to thicken in the southeastern rim of the amphitheater, particularly at the topographic low (*e.g.*, loc. 5 in Fig. 8). The deposit is more than 50 cm thick within 200 m from the rim of the amphitheater.

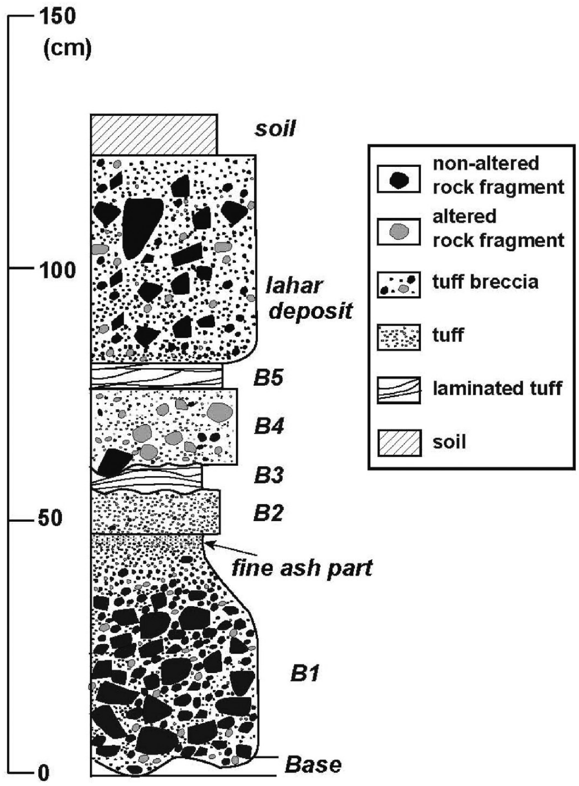

Figure 9. The idealized column of the surge deposits of the AD 1888 eruption, after Fujinawa *et al.* (2008).

Juvenile fragments are not included. The deposit is white to brown, comprising dense rock fragments of various sizes together with lapilli and ash consisting of hydrothermally altered fragments, silica minerals, and clay materials. The total volume of the deposit is estimated as 1x10^7 m^3 (Nakamura and Glicken, 1988). Five distinct beds, B1 to B5, can be observed. These are well observed at loc. 5 in Fig. 8. Figure 9 presents the idealized column.

Figures 10 and 11 present the grain size characteristics. The massive B1, B2, and B4 beds and also the distal facies of the B1 bed are plotted in or near the field for the Mount St Helens basal

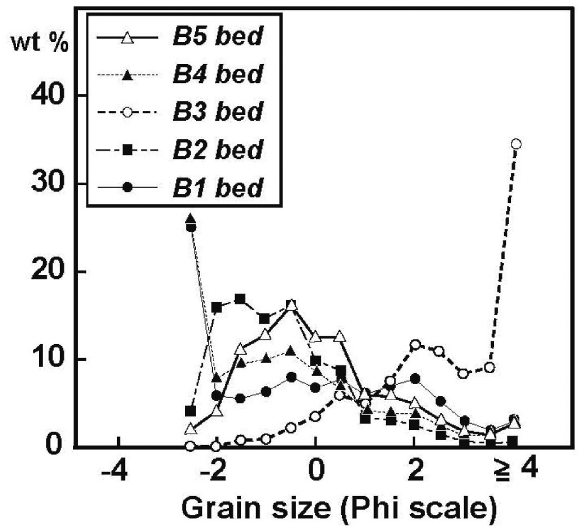

Figure 10. Grain size distribution for the deposits of the AD 1888 pyroclastic surge, after Fujinawa *et al.* (2008).

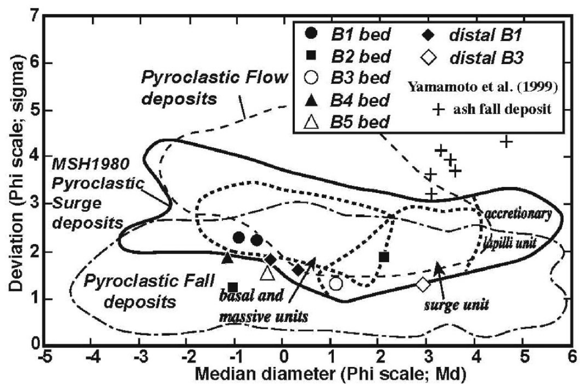

Figure 11. Grain size characteristics for the deposits of the AD 1888 event, after Fujinawa *et al.* (2008).

and massive units (Hoblitt *et al.*, 1981). Both the proximal and the distal facies of the B3 bed are in the field for the Mount St Helens surge unit, whereas the B5 bed plots near the field for the basal and massive Mount St Helens units. The massive deposits are generally suggestive of rapid deposition from high-concentration suspension with little tractional transport (Sohn and Chough, 1989; Nemeth *et al.*, 2001). Based on the distribution and thickness, B1 would be the topographically controlled (or channelized) high-concentration part of a base surge (Hoblitt *et al.*, 1981; Waitt, 1981). This explanation is supported by the clast-supported, openwork, and fine-depleted characteristics of B1. Vesicles of a few millimeters in diameter in the matrix suggest that the bed is the product of a wet surge composed of a three-phase system: particles, gas, and liquid water (Frazzetta *et al.*, 1983). B1 is interpreted to have been deposited from highly concentrated, polydispersive suspension without formation of traction-related bedforms or sorting of different grain sizes by turbulence (Yamamoto *et al.*, 1999). Presumably, the distal facies of B1 deposited from sediment-starved and swiftly moving surge that had been derived from a surge cloud with low concentration and good segregation (Sohn and Chough, 1989). Such a low concentration surge would be produced bipartitely with a highly concentrated underflow by gravitational transformation from a near-vent surge (Chough and Sohn, 1990). The apparent fining upward trend and the fine ash part at the top might have been formed when a stratified density current gradually changed its flow mode from quasi-steady to depletive waning (*cf.*, Kneller and Branney, 1995).

Based on the distribution and thickness of the B2 bed, the topographic control also influenced deposition. The massive nature of B2 implies rapid suspension sedimentation from an unsteady high concentration pyroclastic density current (base surge). Thus, B2 would deposit rapidly from a near-vent surge or high-concentration underflow of a surge lacking sorting and traction transport.

The B3 bed is characterized by planar and locally crossly bedded alteration of well-sorted fine to medium ash layers. These features likely resulted from a turbulent, low-concentration surge with pulsatory depositions (Sohn and Chough, 1989; Nemeth *et al.*, 2001). The sand-wave structures must be controlled by fluctuations in the flow velocity, as reported by Cole (1991). The B3 bed was deposited from a generally low-concentration surge with non-uniform flow existing locally.

The clast-supported nature and openwork texture of B4 suggest a rapid deposition from a near-vent surge or high-concentration underflow at the head of a surge. It is consistent with the observation that B4 deposited preferentially at topographically low areas, and that it contained abundant angular clasts. The bedding sags associated with some blocks are indicative of ballistic emplacement of large clasts.

Planar bedding or cross-bedding along with less topographically controlled distribution of the B5 bed is indicative of deposition from tractional transport beneath a turbulent, low-concentration surge (Chough and Sohn, 1990).

Landslides after the AD 1888 eruption

Two landslide or wall-collapse events transported more than 10^6 m^3 of debris after the AD 1888 eruption. The first event occurred on 9th and 15th May 1938; this was lahar caused by heavy rainfall along with the melting of snow. The total volume of the deposit was estimated at 1.1 x 10^6 m^3. The second event was a debris avalanche that occurred successively from 3rd April to 5th May 1954. The avalanche reached as far as 3 km north and 2 km northeast of the site of the wall collapse. The volume of deposit was approximately 1.5 x 10^7 m^3.

2-4. Petrology

The rocks composing the Bandai volcano commonly belong to medium-K calc-alkaline series. They mostly show porphyritic nature with 18-30 % plagioclase, 5-8 % hypersthene, 0.5-2 % augite and 0.5-1.5 % titanomagnetite as phenocryst phases. Trace amounts (< 01 %) of phenocrystic olivine and/or quartz can be observed in several samples. Hornblende is rarely found in a few lavas. Bulk chemical variation for the rocks of Bandai volcano is quite restricted, with SiO_2 varying from 56 to 63 wt.% of andesitic in composition.

Tholeiitic lava samples were recognized near the bottom (more than 75 m below the ground level) of the boring core drilled at the avalanche valley of northern foothills. The samples are augite- and olivine-phyric basalt. These might be precursory products of the Bandai volcanic activity of 0.72-0.86 Ma (Tanaka *et al.*, 1997).

3. Azuma volcano

3-1. Introduction

The Azuma volcano has a long eruption history, and its eruption products cover an area of ca. 25 km x 15 km. Many peaks can be seen, such as Iegatayama, Issaikyo (1948.8 m), Higashi-Azumayama (1974. 7 m), Azumakofuji (1704.6 m), and Kohyama (1804.8 m) in the eastern part; Shogensan (1892.6 m), Higashidaiten (1927.9 m), Mamamori (1910.2 m), and

Naka-Azumayama (1930.6 m) in the middle part; and Tohjyuhryoh (1860 m), Nakadaiten (1963.6 m),

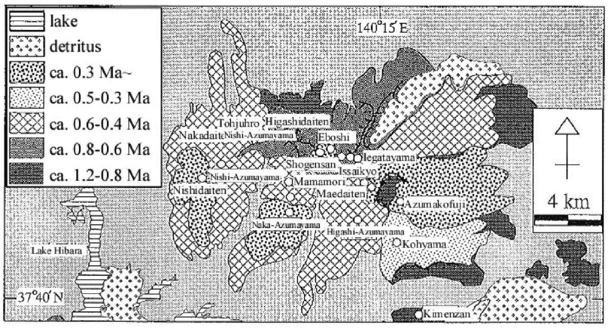

Figure 12. Distribution of eruption products of five periods of volcanic activity in the Azuma volcano.

and Nishi-Azumayama, Nishidaiten in the western part (Fig. 12). The Azuma volcano is not a typical single stratovolcano but a volcano group comprising many small-sized stratovolcanoes (Fujinawa and Kamoshida, 1989).

3-2. Geology

The early studies (*e.g.*, Kawano *et al.*, 1961; Kuno, 1962; NEDO, 1991a) revealed the outline of the geology of the Azuma volcano. Based on the K-Ar data by NEDO (1991a), the volcanic activity can be divided into five periods: 1.2 to 0.8 Ma, 0.8 to 0.6 Ma, 0.6 to 0.4 Ma, 0.5 to 0.3 Ma, and less than 0.3 Ma (Fig. 12). Most of the products are andesitic lava flow, but in the later part of each period, a lava dome or pyroclastic cone tends to be formed in the summit area. Except for the period of 0.5 to 0.3 Ma, the eruption products distributed widely in the area of the Azuma volcano. The newest activity is restricted to the area around Issaikyo to Azumakofuji. This activity began at about 7 ka, and five magmatic phases are recognized (Yamamoto, 2005). These are the Okenuma (ca. 7 to 6.5 ka), Goshikidake (ca. 6.5 to 6 ka), Azumakofuji (ca. 6 to 5 ka), Issaikyo (ca. 5 to 4 ka), and Oana (AD 1331) phases (Yamamoto, 2005). These were series of volcanic eruptions with intermittent phreatic eruptions. Figure 13 shows the generalized columnar section and the location of the craters. The isolated phreatic eruptions are also recognized (Fig. 13). A horseshoe-shaped caldera can be observed in the eastward area of Issaikyo. It was formed some time between 0.28 and 0.1 Ma (Kamoshida, 1991), when the main edifice composed of some small stratovolcanoes in the eastern part of the Azuma volcano had established. Thus, the latest stage would be regarded as the post-caldera stage of the eastern part of the Azuma volcano from the viewpoint of the generalized evolutionary course of the stratovolcano in Japan (Moriya, 1983).

3-3. Historic eruptions

Many historic activities have been recorded in written accounts. Among these activities, from AD 1893 to 1895, two people died on 7th June 1893 (Omori, 1893). In May 1893, phreatic eruptions occurred at Tsubakurosawa on the west of the Oana crater (Yokoyama, 1893) and continued intermittently till 1895. The two people who died were from the meteorological agency. Subsequent activities were recorded in 1914, 1932, 1950, 1952, 1966, 2000, and 2008 to present. Recent activities are characterized by a large-scale gas emission from the Oana crater. The height of the volcanic

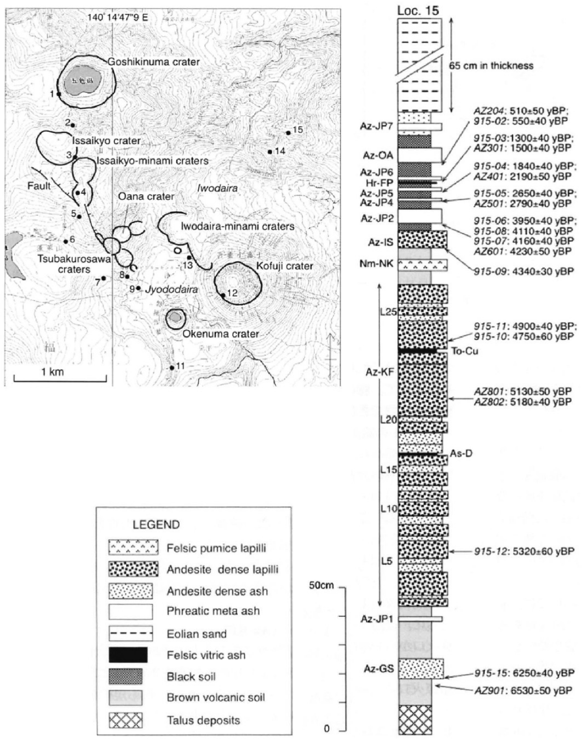

Figure 13. The location of craters and the representative columnar section of tephra layers of youngest activity of the Azuma volcano (Yamamoto, 2005).

fumarole was 70~800 m on 11th November 2008. Moreover, volcanic earthquakes have been frequently observed from 1965, when the Meteorological Agency of Japan started the monitoring at the Azuma volcano. In particular, the frequency of the earthquakes became cyclic from 2001 to 2009 with peaks by two- to three-year intervals (Fig. 14).

3-4. Petrology

Most of the rocks from the Azuma volcano belong to medium-K calc-alkaline andesite, having phenocrysts of plagioclase and two pyroxene with or without olivine and quartz (*e.g.*, Yamamoto, 2005). More specifically, the whole-rock chemical compositions are slightly different by the age and location of the eruption center. The products from eruption centers in the western part tend to have higher incompatible element concentrations. Furthermore, a minor amount of tholeiitic rocks can be observed. Recently, Takahashi *et al.* (2013) examined the genetic relationship between calc-alkaline and tholeiite rocks in detail, and concluded that the calc-alkaline primary magma was derived by the melting of the upper mantle, whereas the tholeiitic one was by the melting of the lower crust.

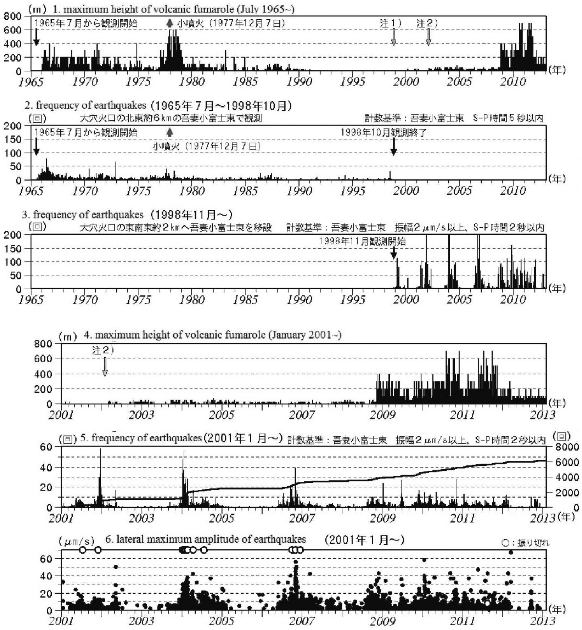

Figure 14. The frequency and lateral maximum amplitude of earthquakes, the maximum height of volcanic fumarole of the Azuma volcano during July 1965 to January 2013 (Sendai District Meteorological Observatory, 2013a).

In terms of the chemical compositions of the latest activity, two distinct variation trends can be observed in Cr and Ni vs. SiO_2 diagrams. The products from the Goshikidake and Oana activities have higher Cr and Ni contents than those from the Azumakofuji and Issaikyo activities (Ban, 2007).

4. Zao volcano

4-1. Introduction

The Zao volcano is one of the representative stratovolcanoes in northeast Japan, situated in the central part of the Quaternary volcanic front of the northeast Japan arc (Fig. 1). The volcanic edifice has many peaks, including Jizosan (1736), Kumanodake (1841), Goshikidake (1674), and Kattadake (1758). These peaks are roughly arranged in the line of northwest to southeast. The Umanose caldera, ca. 2 km in diameter, is in the central part of this volcano. The youngest edifice, Goshikidake, grew from the caldera floor. The present crater lake, Okama, is in the west part of the Goshikidake.

The number of eruption records is highest among active volcanoes in northeast Japan, and there is a long eruption history of ca. 80 my. The activity can be divided into three stages. The latest stage started at about 30 ka, when the Umanose caldera was formed. Most of the eruptions of this stage were explosive, and formed many types of pyroclastic deposits. We will observe a variety of these deposits and understand the change of the eruption features of this volcano during the past ca. 30 ky.

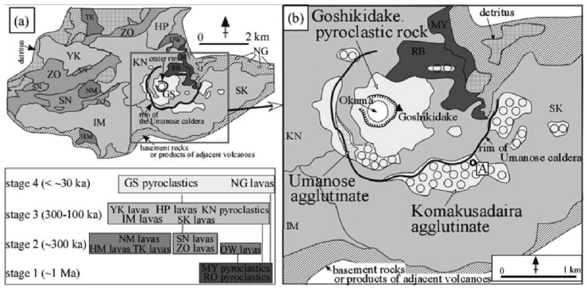

Figure 15. Geologic map of the Zao volcano, after Sakayori (1992) (a), and that of the summit area, after Ban *et al.* (2008) (b).

In frontal volcanoes, calc-alkaline and tholeiitic rocks usually coexist. The rocks of calc-alkaline series are andesite to dacite in many cases, while those of tholeiite are basalt to dacite. In the Zao volcano, a basaltic lava of the calc-alkaline series can be exceptionally observed. This lava was formed at about 100 ka. We will observe this lava flow.

4-2. Geology

Geological and petrological studies of the complete volcanic sequence were performed by Ichimura (1951, 1960), Tiba (1961), Oba and Konta (1989), and Sakayori (1991, 1992). K-Ar dating was performed by Takaoka *et al.* (1989). According to Oba and Konta (1989) and Sakayori (1992), the activity of the Zao volcano is divided into the following stages: ca. 0.8 to 0.6 Ma, 0.4 to 0.1 Ma, and less than ca. 30 ka. Sakayori (1992) divided the

0.4 to 0.1 Ma activity into 0.4 to 0.3 and 0.3 to 0.1 Ma activities. Figure 15(a) shows a simplified geological map of the Zao volcano based on Sakayori (1992).

The eruption products of ca. 0.8 to 0.6 Ma are hyaloclastites, which include bombs showing a pillow-like structure, and are tholeiitic basalt to andesite. Several dykes can also be seen. The heads of the dykes dispersed to be trains of bombs have a quench structure. These eruptions would have taken place under lake water.

During ca. 0.4 to 0.1 Ma, andesitic to dacitic lava flows swelled out from many vents arranged from northwest to southeast. Lava flowed down both eastward and westward. The lava interbedded with associated pyroclastic rocks near the summit area. Vulcanian eruptions would have been the major mode of eruption in this stage.

The most recent stage of the Zao volcano began at about 30 ka, and numerous small to medium-sized explosive eruptions of calc-alkaline basaltic andesite magmas have occurred since then. At about 30 ka, the horseshoe-shaped Umanose caldera (1.7 km in diameter) was formed. A small cone, Goshikidake, formed subsequently in the inner part of the caldera. The Crater Lake Okama is located in the cone.

The Goshikidake pyroclastics are the main products of the most recent stage, and are divided into Komakusadaira agglutinate (ca. 32 to 13 ka), Umanose agglutinate (ca. 7.5 to 4.1 ka), and Goshikidake pyroclastic rock (ca. 2.0 ka to present) (Ban *et al.* 2008; see Figs. 15 (b) and 16). The ages are estimated by correlation to the tephra layers. Imura (1999) recognized 10 tephra layers for the most recent stage of Zao, and Ban *et al.* (2005) and Miura *et al.* (2008) re-examined the tephra stratigraphy and recognized 16 layers. The first four of them (Z-To 1 to 4) correlate to Komakusadaira agglutinate, the next six (Z-To 5a, 5b, 5, 6, 7 and 8) to Umanose agglutinate, and the others (Z-To 9 to 14) to Goshikidake pyroclastic rock. The Komakusadaira agglutinate can be further divided into Kumanodake agglutinate, Komaksadaira pyroclastic rocks, and Kattadake pyroclastic rocks (Takebe and Ban, 2011). The Goshikidake pyroclastic unit is mainly made up of pyroclastic surge deposits and can be divided into five units. Figure 16 shows the idealized columnar section of tephra layers at the summit area and the eastern foot of the Zao volcano by Ban *et al.* (2005).

4-3. Historic eruptions

From the record of AD 773, many historic activities were recorded in written accounts. Among the activities from AD 1894 to 1895, phreatic eruptions occurred on 15th and 19th February, 22nd August, and 27th–28th September 1895, with several precursory vulcanian eruptions during February to July 1894. All were generated at the Okama crater lake. The last one was the climatic eruption. The eruption column reached a height of ca. 350 m (Fig. 17) (Fujinawa *et al.*, 2008; Miura *et al.*, 2012).

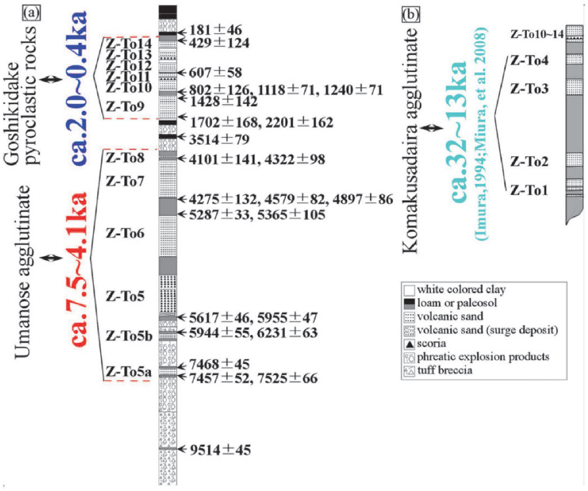

Figure 16. Idealized columnar section of tephra layers at the summit area (a) and the east foot (b) of the Zao volcano, after Ban *et al.* (2005) partly modified and English translated.

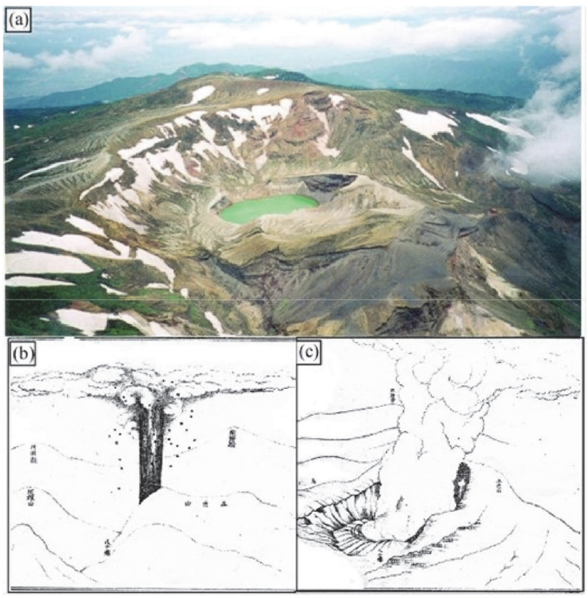

Figure 17. An aerial photo of the Goshikidake and Okama (a), a sketch map of the climax eruption on 27th September (b), and a sketch map of the fumarole on 6th October (c).

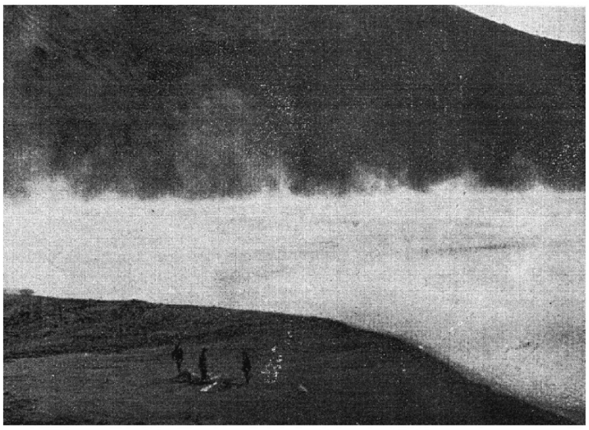

Figure 18. A photograph of crater lake Okama in November 1939 by Anzai (1961).

The latest volcanic activity occurred during 1939 to 1940. Steam rising from the crater lake was sometimes observed (Fig. 18), and in October 1939 and March 1940 the lake was partly covered by sulfur, which would be precipitated from the fumarole. The depth of the lake was ca. 40 m with a bowl-like shape in July 1939, but it became deeper up to ca. 62 m in November 1939. We do not have any evidence that solid materials erupted from Okama, but a very small amount of mud flow poured out from new fumarole formed ca. 500 m northeast of Okama in April 1940 (*e.g.*, Anzai, 1961).

4-4. Petrology

The rocks from the oldest stage belong to the tholeiitic series, while those of the other stages belong to the calc-alkaline series. The calc-alkaline series rocks from different eruption periods usually show slight differences in chemical composition, as in potassium levels. Sakayori (1992) showed that the tholeiitic rocks were formed by fractional crystallization from basaltic magma, while the calc-alkaline rocks were formed by mixing between mafic and felsic magmas. This mafic magma has large-ion- lithophile contents that are similar to those of rear arc volcanoes and different from the Zao tholeiitic basalts. Further, Tatsumi *et al.* (2008) showed that calc-alkaline mafic magmas, having higher concentrations of incompatible elements, are isotopically depleted, while tholeiitic basalts, having lower concentrations of incompatible elements, are isotopically enriched. Coupled with the results of the micro-analyses of phenocrysts, they deduced that the primary magma of the calc-alkaline series was formed by the melting of the upper mantle, while that of the tholeiitic series was by the lower crust.

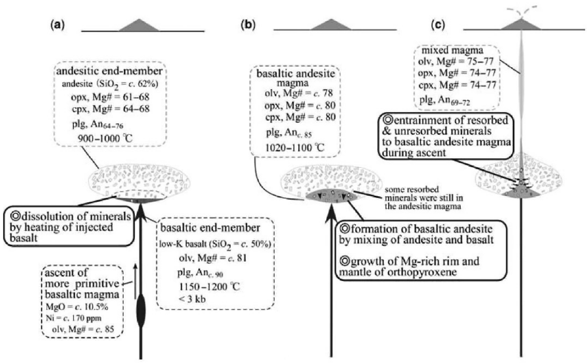

Figure 19. Schematic representation of the magmatic processes involved in the generation of Z-To5, after Ban *et al.* (2008). An, anorthite; Mg#, 100 x [Mg/(Mg + Fe)]; opx, orthopyroxene; cpx, clinopyroxene; olv, olivine; plg, plagioclase.

In terms of the evolution of the magma feeding system, high-resolution analysis has been performed on the activities of the most recent stage (Ban *et al.*, 2008). The magma feeding system consists of felsic magma, which ponded in the shallow chamber, and mafic magmas, which repeatedly ascended from depth and infused into the shallow chamber. The resultant mixed basaltic magmas erupted. Figure 19 shows, as an example, the evolution of the magma feeding system for ca. 5.8 ka activity. Both the mafic and felsic magmas change their compositions during a single activity. The evolution courses are various by activities.

5. Sengan volcanic field (Iwate, Hachimantai, Akita Yakeyama, and Tazawako)

The Sengan volcanic field (40°N, 141°E) is a volcanic cluster consisting of a number of basalt-andesite stratovolcanoes and caldera-related ignimbrite (Fig. 20). The field is one of the volcanic clusters lying on the volcanic front of the northeastern Japan arc with the intervals of about 80 km. This clustering of volcanoes relates to the locally developed finger-like hot regions within the mantle wedge (Tamura *et al.*, 2002). The Sengan volcanic field is the largest of these clusters, covering an area of about 1000 km^2. In the area, caldera-related ignimbrite sheets and lava from andesitic and basaltic volcanic cones complexly overlap each other. The volcanic cluster has developed for ca. 3 million years, with the eruption centers moving. Although more than 50 volcanic centers were identified, most volcanic edifices were obscured by erosion, coalescence with contiguous cones, and covering by ignimbrite and younger lavas. At three of these cones, Akita-Komagatake, Akita-Yakeyama, and Iwate, magmatic eruptions have occurred during the last 10 ky.

ignimbrite from calderas and cone-forming lavas of basalt, andesite, and dacite. Old andesitic lavas (3 -

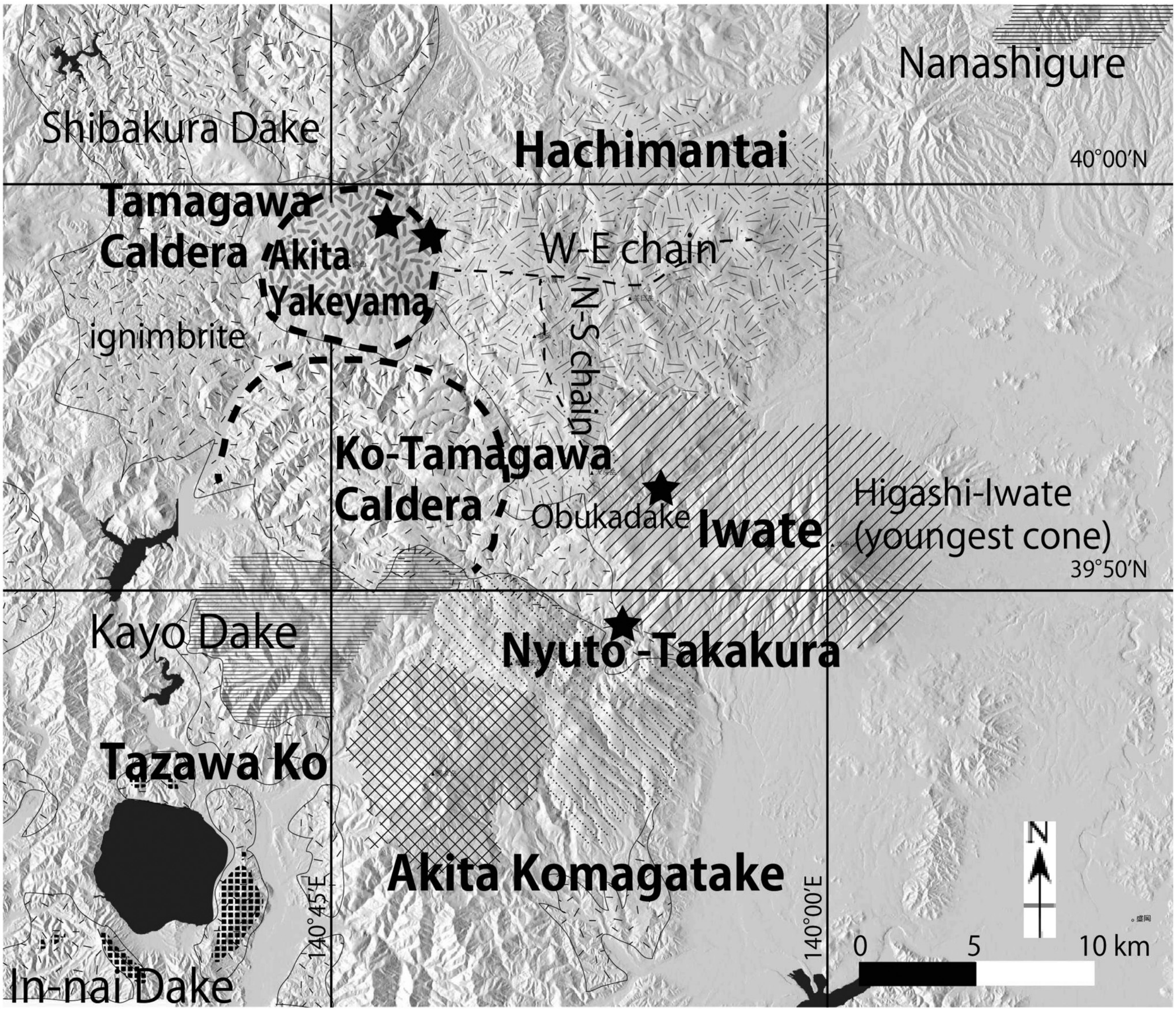

Figure 20. The outline map of the Sengan volcanic field. Hatching parts are Quaternary volcanoes. Thick broken lines indicate caldera rims. Thin broken lines are chains of stratocones. Stars are the locations of geothermal power stations.

Conventionally, the volcanic field is divided into nine volcanoes: Akita-Yakeyama, Hachimantai, Nanashigure, Ko-Tamagawa caldera, Tamagawa caldera, Iwate, Tazawako caldera, Kayo-dake, Nyuto-Takakura, and Akita-Komagatake. The extent of each volcano varies from author to author: some regard a single cone as a volcano, whereas others consider a volcano encompassing a broad area involving separated cones of different ages. For example, Kawano and Aoki (1959) included the Nyuto-Takakura volcano in Akita-Komagatake, whereas Fujinawa *et al.* (2004) limited the extent of Akita-Komagatake to the newest cone.

The volcanic field is mostly composed of

1 Ma) occur in eroded, obscured cones (Kayo-dake, In-naidake, Shibakura-Dake, Obukadake, etc.) and in the underlayer beneath younger cones (Matsukawa Andesite) (Uemura, 1987; Suto, 1992). Ignimbrite layers (Tamagawa welded tuff and Ko-Tamagawa welded tuff) from two calderas (Tamagawa and Ko-Tamagawa calderas) broadly distribute over the field. The eruption ages of the Tamagawa and Ko-Tamagawa calderas are 1 Ma and 2 Ma, respectively. A recent study elucidated that the lake Tazawa-Ko, located in the southwest of the field, is also a caldera formed by an ignimbrite eruption ca. 1.4 Ma (Kano *et al.*, 2007). Most of the distinct volcanic edifices are composed

of lavas younger than 1 Ma, overlying the ignimbrite or the 1 to 3 Ma andesite. Hachimantai, Nanashigure, and Nyuto-Takakura are extinct volcanic groups that consist of some small cones with eruption ages widely ranging from ca. 1 Ma to 0.1 Ma (Ban *et al.*, 1992; Suto, 1984; Suto *et al.*, 1990; Ohba and Umeda, 1999; Ohba *et al.*, 2003). Iwate, Akita-Yakeyama, and Akita-Komagatake are the youngest volcanic cones in the field. The Iwate volcanic group is a W-E oriented volcanic chain where magmatic activity has shifted from west to east for ca. 0.8 Ma (NEDO, 1991b). The prominent easternmost cone has been built for the last 30 ka by basaltic activities. The flank effusion of basaltic andesite magma in AD 1732 (Yakihashiri Lava) is one of the historical eruptions. Akita-Komagatake is a young basaltic stratocone that has a caldera and craters on the top where younger cinder cones are distributed. The volcanic activity commenced ca. 100 ka and the last eruption occurred in 1970. Akita-Yakeyama is a young andesitic stratocone filled in the caldera collapsed by the eruption of the 1 Ma Tamagawa welded tuff. There are some dacitic lava domes in the central crater and on the flank of the cone.

The Sengan volcanic field is a well-known geothermal field, where many geothermal power plants have been built and surface manifestations of geothermal activities can be seen everywhere as warm ground, geysers, hot springs and fumarole. There are many hot spring resorts which tourists visit for relaxation. The hot springs are geochemically diverse, as pointed out by Shigeno and Abe (1987), who classified them into six types: acid Cl-SO_4, acid SO_4, neutral Cl, neutral Cl-SO_4-CO_2, neutral Cl-SO_4, and neutral CO_2 type hot springs. There are four geothermal plants in the field: Matsukawa (23.5 MW), Onuma (9.5 MW), Kakkonda (50 MW), and Sumikawa (50 MW). A total of 133 MW account for 24% of nationwide geothermal power. Hydrothermal alteration zones are distributed throughout the field, not only in the volcanic centers but in valley bottoms where Neogene basement rocks are exposed. Distinct acid alteration zones scattered throughout the field are characterized by the presence of pyrophyllite, alunite, dickite, and kaolinite (Kimbara, 1987).

6. Iwate volcano

6-1. Introduction

The Iwate volcano is one of the representative large stratovolcanoes in northeast Japan, located ca 15 km northwest of Morioka city. The volcanic edifice is divided into eastern and western parts, the Higashi-Iwate and Nishi-Iwate volcanoes. The Higashi-Iwate volcano is a conical-shaped stratovolcano with the highest peak at Yakushidake (2038 m). Yakushidake has a crater 500 m wide. Behind the Higashi-Iwate volcano is the Nishi-Iwate volcano, which has a summit caldera (Nishi-Iwate caldera) ca. 2.5 km wide from east to west and ca. 1.5 km wide from north to south. A central cone with a crater lake, named Tazawa-Ko, can be seen in the caldera.

6-2. Geology

Many researchers, such as Onuma (1962), Nakagawa (1987), and Doi (2000), have investigated the geologic features of the Iwate volcano. The most recent study is by Itoh and Doi (2005), who revealed a detailed stratigraphy of this volcano (Fig. 21). The following summarizes the results of their study. The Iwate volcano has repeatedly experienced the contruction and destruction of volcanic edifices. The activities of Higashi- and Nishi-Iwate started at about 0.13 Ma and 0.3 Ma, respectively, and have continued to the present (Fig. 21). The activities of Higashi- and

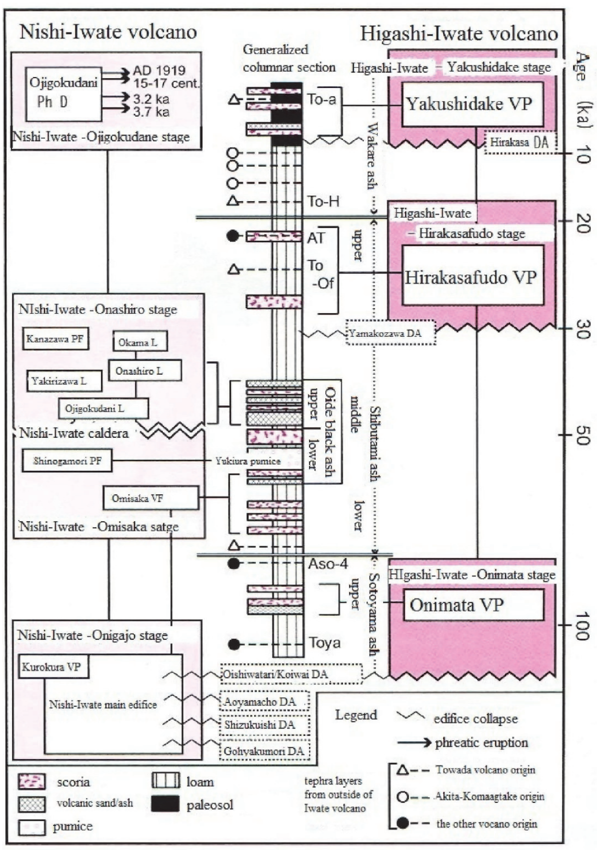

Figure 21. Volcanic stratigraphy of the Iwate volcano, after Itoh and Doi (2005): English translated version.

Nishi-Iwate volcanoes are not separated but rather coeval at least past 0.1 my.

The activity of Nishi-Iwate is divided into four stages: Onigajo (ca. 0.3 to 0.1 Ma), Omisaka (ca. 80 to 50 ka), Onashiro (ca. 50 to 28 ka), and Ojigokudani (ca. 7 ka to present). The main part of the Nishi-Iwate volcanic edifice was formed in the Onigajo stage. The eruption products are andesitic lava and associated pyroclastic rocks. During the construction of the edifice, sector collapses occurred at least four times. After a ca. 20 ky dormancy, the activity of the Omisaka stage started. Andesitic lava flows distributed toward the southwest, and calc-alkaline andesitic to dacitic pyroclastic flows deposited southward. Subsequently, the Nishi-Iwate caldera was formed in the summit area at the beginning of the Onashiro stage. Thereafter, andesitic lava and associated pyroclastic rocks were discharged from vents in the inner parts of the caldera. As a result, a small andesitic cone that has a summit crater and a much smaller post crater cone have formed. In the Ojigokudani stage, relatively large phreatic eruptions occurred four times during the past ca. 7 ky (Itoh, 1999).

The activity of Higashi-Iwate is divided into three stages: Onimata (ca. 0.12 to 0.09 Ma), Hirakasafudo (ca. 30 to 20 ka), and Yakushidake (ca. 7 ka to present). During the Onimata stage, a stratocone, composed of basaltic lava flows and associated pyroclastic rocks, grew in the inner part of the caldera, which was formed in the later part of the Nishi-Iwate Onigajo stage. At ca. 30 ka, the beginning of the Hirakasafudo stage, the stratocone and eastern part of the Nishi-Iwate edifice collapsed, forming a caldera. Another basaltic stratocone (Hirakasafudo edifice) grew in the inner part of the caldera until ca. 20 ka. The initiation of the latest Yakushidake stage was the collapse of the Hirakasafudo edifice and formation of a debris avalanche at ca. 7 ka. The debris avalanche flowed down the Kitagami river and reached to the area of the present-day downtown of Morioka city. The inner part of the caldera, the newest basaltic stratocone, has been growing until the present day.

6-3. Historic eruptions

After the 17th century, many historic activities were recorded. Most of these were eruptions or small-scale collapses of Yakushidake and phreatic eruptions in the Ojigokudani area. Among these, the AD 1686, 1732, and 1919 eruptions have been well investigated through the examination of written accounts coupled with eruption products (Itoh, 1998; Doi, 2000). In AD 1686, the eruption started with the phreatomagmatic eruption from the summit crater, forming lava flow and scoria emission, and subsequently the pyroclastic surge and debris flow were generated. The ash fall was observed in Morioka city. In 1732, basaltic lava (Yake-bashiri lava flow) swelled out from three linearly arranged scoria cones (1030 to 1130 m a.s.l.) formed on the northeastern flank of Yakushidake. At around 1170 m, two other scoria cones were formed, and very thin lava flowed out (Togari and Nakagawa, 1998). The AD 1919 activity was a series of small phreatic explosions at Ojigokudani.

Volcanic seismic activity at the Iwate volcano increased in 1998. In September 1995, deep volcanic tremors with a duration of 45 minutes were observed at depths of 8-10 km beneath the eastern flank. From 1996 to 1997, weak seismic activities and tremors were observed. The shallow and deep seismic activities and crustal deformations started in the middle of February 1998 and increased until 5th September 1998, when a M 6.1 tectonic earthquake occurred at ca. 10 km southwest of the Iwate volcano. After this, the number of shallow volcanic earthquakes gradually decreased. In turn, volcanic fumarole activity became intense in Ojigokudani in Nishi-Iwate from May 1999, which continued to 2000 (Fig. 22). This area was red taped until July 2004.

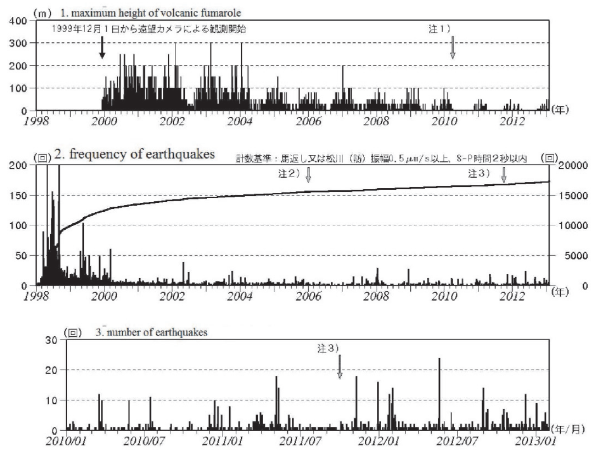

Figure 22. The frequency of earthquakes, the height of volcanic fumarole of the Iwate volcano from 1998 to 2013 (Sendai District Meteorological Observatory, 2013b).

It was inferred that this seismic activity was caused by dike intrusions beneath the Iwate volcano. Magma ascended beneath the Higashi-Iwateste stratocone and later migrated laterally westward but did not erupt (*e.g.*, Nishimura *et al.*, 2000; Tanaka *et al.*, 2002).

6-4. Petrology

Most of the rocks from the Iwate volcano belong to low-K tholeiitic basalt to basaltic andesite, having phenocrysts of plagioclase, olivine with or without clinopyroxine and orthopyroxene (*e.g.*, Ishikawa *et al.*, 1982; Nakagawa, 1994; Nakagawa and Togari, 1999). A subordinate amount of calc-alkaline andesite to dacite can be observed. All of the rocks of Higashi-Iwate belong to the tholeiitic series, while some of Nishi-Iwate belong to the calc-alkaline series. The tholeiitic rocks can be divided into two types: silica richer and poorer. It was inferred that the latter was differentiated much more deeply than the former (Nakagawa, 1994). The calc-alkaline rocks were formed by mixing between tholeiitic basaltic magma and felsic magma in the shallow crustal level. It would be probable that the shallow chamber existed beneath Nishi-Iwate but not beneath Higashi-Iwate (Fig. 23) (Nakagawa and Togari, 1999).

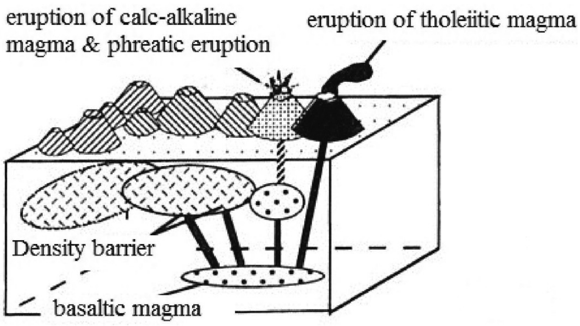

Figure 23. Schematic representation of the distribution of shallow magma chambers (Nakagawa and Togari, 1999).

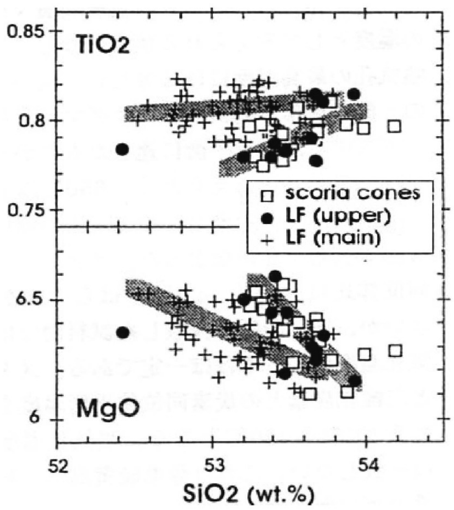

Figure 24. Selected Harker diagrams of rocks of the AD 1732 activity in the Iwate volcano, after Togari and Nakagawa (1998).

The eruption products of AD 1732 are tholeiitic basaltic andesite, with ca. 52.5% to 54.2% in SiO_2 content. The compositions of rocks of the upper scoria cone and associated thin lava flow differ from those of the linearly arranged three scoria cones and Yake-bashiri lava flow (Fig. 24) (Togari and Nakagawa, 1998).

7. Hachimantai Volcano

7-1. Introduction

The Hachimantai volcano is an "active volcano" or Katsu-kazan according to the definition by the Japan Meteorological Agency (JMA). To avoid confusion, it is important to note that the JMA definition of active volcanoes as "volcanoes which have erupted within 10 ky or volcanoes with vigorous fumarolic activity" does not require any magmatic eruption record. Hachimantai satisfies the requirement in two respects: fumarolic activity is intense on the western flank and in the southern valley of Hachimantai cone (sensu stricto), and a non-juvenile hydrothermal eruption occurred at the summit of Hachimantai ca. 6 ky. However, magmatic eruptions have never happened since ca. 100 ky (Ohba and Umeda, 1999).

7-2. Geology

The Hachimantai volcano consists of coalescing volcanic cones forming two volcanic chains trending the W-E and N-S directions. The highest peak of Hachimantai (Hachimantai sensu stricto; 39.955°N, 140.857°E, 1614 m) is located at the intersection of these chains. The N-S volcanic chain is 10 km long, consisting of the cones of Hachimantai, Mokkodake, Morobi-dake, No name peak (1481 m peak), Kensomori, and Obuka-dake from north to south. The chain is connected to the curved volcanic chain in the western end of the Iwate volcano sensu lato. The cones in the N-S chain are small hills with shallowly sloping sides, except for Mokko-dake which is a jagged dome with distinct lava flows on the flank. This volcanic chain was mostly formed by the eruptions of medium-K andesitic magma in the period between 1.0 and 0.7 Ma (Ohba *et al.*, 2003). The W-E chain is 15 km long, consisting of the cones of Fukenoyu, Hachimantai, Gentamori, Chausudake, Ebisumori, Daikokumori, Yanomunedake, Nishimori-Yama, and Maemori-Yama from west to east. Akitayake-Yakeyama is located on the western extension of this W-E chain. Volcanic cones of the eastern part of this chain are clearly conical, although the shapes of some cones have been obscured by landsides, erosion, and coalescence with contiguous cones. From Hachimantai to Maemori-Yama, volcanic activities shifted from west to east between 0.7 and 0.1 Ma, whereas in the west, volcanic activity migrated from Hachimantai via Fukenoyu to the western extension where the presently active Akita-Yakeyama is (Ohba and Umeda, 1999; Suto and Mukoyama, 1987).

7-3. Prehistoric hydrothermal eruptions

Distinct volcanic craters are topographically well preserved at the top of Hachimantai sensu stricto (Fig. 25). At least 20 craters are densely distributed on the summit plateau, forming some crater chains. The craters range from several meters to 180 m in diameter, and the longest crater chain is about 1.5 km long. Many of the craters are filled with water, forming round, gourd-shaped (Gama numa), or elongated ponds (Hachiman numa). The crater chains dominantly trend in the W-E direction, which is parallel to the line of the south-facing cliff in the south of summit plateau.

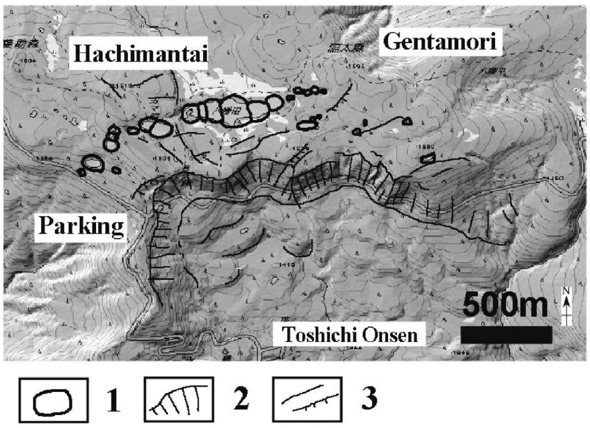

Figure 25. Hydrothermal explosion craters on the summit plateau of Hachimantai. Legends; 1: hydrothermal explosion crater, 2: landslide scars, 3: cracks.

The craters were formed by non-juvenile hydrothermal eruptions. Because the magmatic eruptions of Hachimantai sensu stricto ceased ca. 0.7 Ma, the formation of the craters are not attributed to magmatic eruptions. In fact, Wachi et al. (2002) found the non-juvenile volcanic ash layers erupted from the craters more than 9 ka, 9-7 ka, and 6 ka. On the basis of topographic observation, Doi (2010) interpreted the origin of the hydrothermal eruptions as the decompression-induced bumping of superheated fluid triggered by a huge landslide. The southern cliff is the main scarp of a huge landslide, the main body of which slid down to the south. As the hydrothermal craters are situated along the crown cracks of this landslide, the formation of the crater or the origin of explosions was related to the landslide. By a sudden removal of overburdened rocks by the landslide, confined superheated fluid was decompressed to explode along the crown cracks. Doi (2010) inferred the same process for topographically similar crater swarms at the Kurikoma volcano. This type of landslide-triggered hydrothermal eruptions is possibly a general phenomenon.

7-4. Petrology

Rocks from Hachimantai are all subalkaline rocks dominated by two rock types: low-K tholeiitic basalt and medium-K calc-alkaline andesite. In the west to the middle of the W-E chain, large cones (Hachimantai, and Chausudake) are composed of medium-K andesite lavas. Minor dacite occurs in small edifices: Fukenoyu and Gentamori (Ohba and Umeda, 1999). Eastern cones (Marmori-Yama and Nishimori-Yama) are composed of low-K tholeiitic basalt (Ohba *et al.*, 2009). The Ebisumori and Daikokumori cones, located midway between medium-K andesitic cones and low-K basaltic cones, consist of magnesian medium-K basaltic andesite that was formed by mixing between the medium-K andesite and the low-K basalt magmas (Ohba *et al.*, 2007a).

8. Akita Yakeyama volcano

8-1. Introduction

Akita Yakeyama is one of the active volcanoes in the Sengan volcanic field. The volcano consists of an andesitic stratocone and minor dacite lava domes. No magmatic eruptions were recorded in historical age, but documented eruptions were all phreatic eruptions or hydrothermal eruptions. Hydrothermal activity is intense all over the volcanic edifice, as surface manifestations are distinct everywhere, such as warm ground, fumarole, and hot springs. In 1997, hydrothermal eruptions occurred twice, one at the northeastern flank on 11th May and the other at the summit on 16th August. The eruption in May was triggered by a landslide that occurred near a hot spring. In the last eruption in August, 3,000 m^3 of mud were discharged from two craters (Ohba *et al.*, 2007b) at the summit.

8-2. Geology of Akita Yakeyama

Akita Yakeyama is an andesitic stratovolcano 7 km in diameter, with andesitic parasite domes and dacitic central domes. The stratocone has a 1 km central crater where the newest lava dome (Onigajo lava dome) is situated at the center and the older lava dome (Tsugamori-Nishi lava dome) on the southeastern rim. Parasitic andesite lava domes and associated lava flows are situated on the eastern flank (Kunimidai) and southern flank (Kuroishimori). The two dacitic lava domes are dissected by explosion craters. The main stratocone surface is shelving: the average of slope angle is only ca. 10° and even the maximum is 16°. The surface of the main stratocone topographically comprises thin lava flows. At the rim of the stratocone, the lava flows are dissected by landslide scarps and gullies. Lavas from the parasitic domes are thicker than the stratocone-forming lavas.

The volcanic edifice has developed since ca. 0.5 Ma within the 7 km caldera collapsed by the eruption of Tamagawa ignimbrite 1 Ma. The volcanic products of Akita Yakeyama partly intercalate with caldera lacustrine sediments, suggesting that the volcanic activity commenced in the caldera lake. The lake was buried outward by andisitic lavas from the central vent. During the post-stratocone-forming period, the parasitic dome and central domes were formed by eruptions of felsic andesite and dacite magmas. The Onigajo lava dome was formed ca. 5 ka (Takashima and Honda, 1985). In this period, explosive activities often occurred to form distinct explosion craters around the summit. Two volcanic ash layers (Ay-3 and Ay-2) from the craters were dated to be ca. 30 ka and 1.4 ka, respectively (Tsutsui and Ito, 2002). Small craters surrounding the Onigajo dome are considered to have been formed by recent hydrothermal explosions.

Hydrothermal activity is distinct at the Akita-Yakeyama volcano. The activity is especially expressed as fumarole, hot spring, sulfur deposition, and warm ground around the summit crater, in the upper parts of heavily eroded radial gullies, at the western foot (Tamagawa hot spring), and along the N-S trending rivulets at the eastern foot (Goshogake, Onuma, and Sumikawa hot springs). These areas are marked by distinct unvegetated ground.

8-3. Historic eruptions

In 1997, hydrothermal eruptions occurred twice: one at the northeastern foot on 11th May and the other at the summit crater on 16th August. Before these eruptions, more than eight historic eruptions (1678, 1867, 1887, 1890, 1929, 1948, 1949, and 1957 A.D.) had been recorded since the 17th century (Murayama, 1973; Tsutsui and Ito, 2002). The volcanic ash layer from the historical eruption in 1678 (Ay-1) was identified by Tsutsui and Ito (2002). All of the historic eruptions were non-juvenile hydrothermal eruptions.

On 11th May 1997, a landslide occurred at the northeastern foot where two hot spring hotels, Sumikawa and Akagawa, were located. A total of 5.1 x 10^6 m^3 of landslide mass slid down 50-70 m to the north. The landslide mass buried the hotel buildings of Sumikawa hot spring where a hydrothermal explosion occurred right after the landslide. Debris then flowed along the Akagawa valley and devastated the hotel of the Akagawa hot spring.

The 1997 summit eruption occurred three months after the landslide-triggered hydrothermal

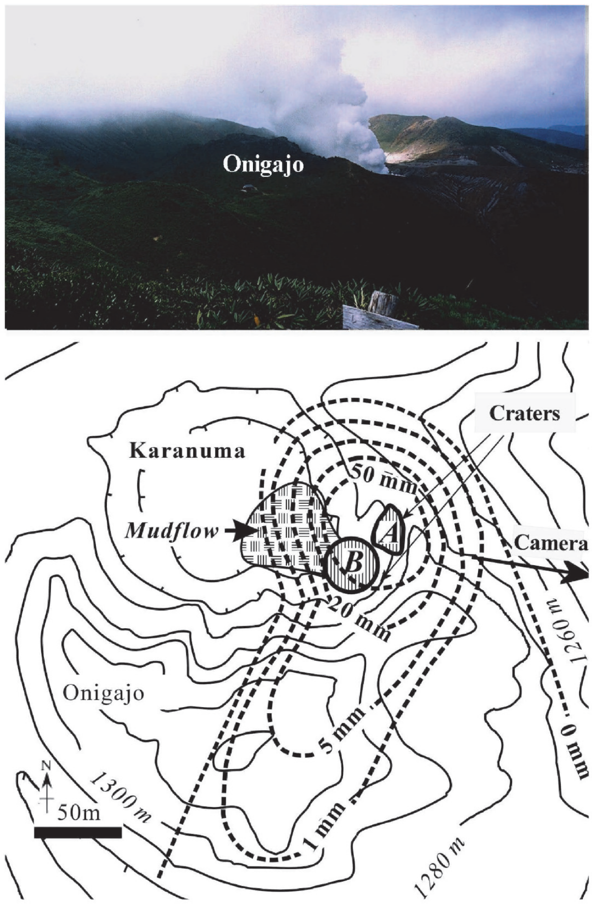

Figure 26. The hydrothermal eruption at Akita Yakeyama on 16th August 1997. The upper photo is taken by a visitor. Photo courtesy of Mr. Fujii, Hanamaki city. The lower figure is the distribution map of craters and eruption products. Dashed lines are isopachs of the air fall deposits.

eruption. At around 10:50 on 16th August, a hydrothermal eruption commenced at the southeastern rim of the Karenuma crater. The eruption occurred at two craters: mudflow effused from one crater, and a discrete explosion occurred at the other crater (Fig. 26). The eruption lasted about 70 minutes. A total of 3000 m^3 of mud were discharged from the craters. The mud consisted of hydrothermal minerals (smectite, silica minerals, kaolinite, pyrophyllite, gypsum, etc.), altered rock, and fresh dacitic lithic fragments. The mud was derived from the sub-volcanic acid hydrothermal system with temperatures higher than 320°C (Ohba *et al.*, 2007b).

8-4. Petrology

Rocks from Akita Yakeyama are dominant medium-K andesite and minor medium-K dacite. The stratocone is exclusively composed of medium-K andesite that contains plagioclase, orthopyroxene, augite, magnetite, and olivine as phenocryst minerals. Quartz phenocrysts occasionally occur as embayed anhedral crystals. The andesite contains abundant evidence of open-system crystallization such as disequilibrium mineral assemblages, e.g., coexistence of iron-rich reversely zoned pyroxene and Mg-rich normally zoned olivine. Ohba (1993) inferred from the mineralogy and whole-rock chemistry that the andesite magma was produced by magma mixing. Dacitic rocks occur in central domes and a parasitic dome. The dacite contains plagioclase, quartz, orthopyroxene, augite, and magnetite as phenocryst. Dacite samples from the Tsugamori Nishi lava dome contain magnesian olivine regardless of its high silica content (69 wt%SiO_2).

9. Tazawako caldera

9-1. Introduction

It was only five years ago that lake Tazawa-Ko was proven to be a caldera lake. The origin of Japan's deepest lake, Tazawa-Ko (423.4 m deep), had been argued for more than half a century. It seems that there were some possible origins, including caldera, meteorite crater, and tectonic-origin. The lake is circular, funnel-shaped, and surrounded by somma-like mountains that consist of volcanic rocks. Although these characteristics suggest the possibility of a caldera, this had not been proven because eruption products had not been found. From geological survey and dating ages, Kano *et al.* (2007) inferred that Tazawa-Ko was formed by an ignimbrite eruption in the period between 1.4 and 1.7 Ma.

9-2. Geology

The lake is surrounded by somma-like mountains consisting of basaltic and andesitic lavas. The volcanic rocks overlie the 2 Ma ignimbrite from the Ko-Tamagawa caldera. The dating ages of somma rocks range from 1.6 to 2.2 Ma. In the lake bottom there are two submerged post-caldera lava domes, Tatsuko-Tai and Shinko-Tai. An andesite sample from Tatsuko-Tai was dated as 1.7 to 1.8 Ma. Ignimbrites are broadly distributed around Tazawa-Ko; stratigraphy, however, has not been well established because of the similarity in lithology of different units from different calderas (2 Ma ignimbrite from Ko-Tamagawa caldera, 1 Ma ignimbrite from Tamagawa caldera, and others). Kano *et al.* (2007) described an ignimbrite that is sandwiched between the 2 Ma ignimbrite from Ko-Tamagawa caldera and the 1 Ma ignimbrite from Tamagawa caldera around Tazawa-Ko. The fission track (FT) ages range from 1.4 to 1.8 Ma, which is a similar range with the K-Ar ages of the somma volcanic rocks. They inferred that this ignimbrite was discharged from the Tazawao-Ko caldera.

10. Quaternary volcanoes in the western Oga Peninsula

10-1. Introduction

In the Oga peninsula, which projects west into

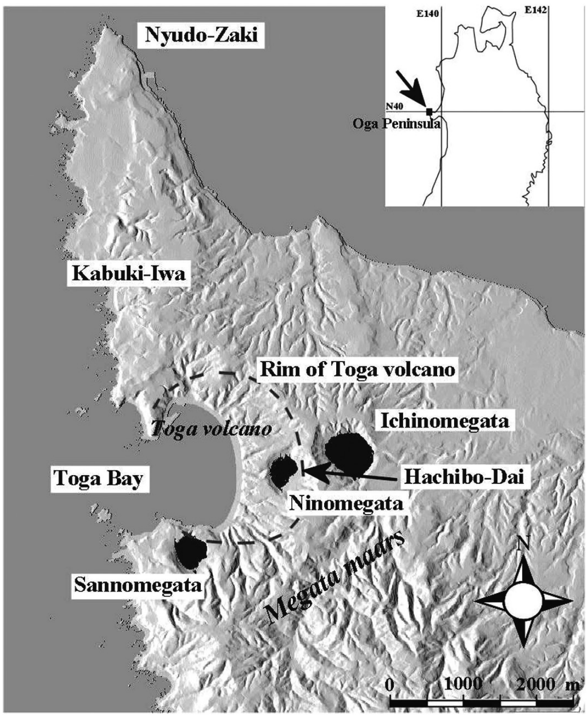

Figure 27. Quaternary volcanoes near the northwestern coast of the Oga Peninsula, Akita, northeast Japan.

the Sea of Japan, there are some small Quaternary volcanoes. Near the base of the peninsula is Kampuzan (355 m high), a small andesitic stratovolcano with two craters on the top. The stratovolcano is about 0.6 km^3 in volume, mostly consisting of andesitic lavas. Near the western coast of the peninsula are three maar volcanoes (Megata maars) and a tuff-ring (Toga) (Fig. 27). These maar and tuff-ring volcanoes are distributed in a small area of 3 km x 4 km. Volcanic products from one of the maar volcanoes contain abundant mantle xenolith, and a number of petrological studies have been carried out. The Toga tuff-ring was identified as a Quaternary volcano in 1999 by Kano *et al.* (1999). From the presence of pumice deposit around the Toga bay, some authors had pointed out for more than half a century that the bay might be an explosion crater. However, many geologists were skeptical about the view because the rounded pumice and the sandy-muddy matrices in the deposit looked like sedimentary rock.

10-2. Geology

Toga volcano

Toga volcano is located in the northwestern coast of the peninsula. As the tuff ring opens to the sea in the west, the bottom of the crater is filled with sea water to form a bay (Toga Bay). The topographic expression of the volcano is a depression with a diameter of 2 km. The bay is located in the west of the depression, and the eastern half of the depression is a steep slope. Kano *et al.* (2002) elucidated from a detailed geological survey that the volcano was a tuff-ring, although original morphology has been obscured by erosion.

Eruption products are distributed in and around the volcano. They consist of lapillistone, lapilli tuff, and tuff comprising juvenile pumice clasts, ash, and accidental lithic fragments derived from basement rocks. Some parts of the deposits are massive, whereas the others exhibit various kinds of traction structures, including parallel, wavy, ripple, and low-angle cross laminar. Kano *et al.* (2002) classified the lithofacies into seven facies (TF1–TF7), and inferred that most of them indicate settlements in water as turbidity currents. The shapes of volcanic glass shards are platy or blocky, implying that their origin is of phreatomagmatic eruption. The phreatomagmatic eruption occurred right beneath the water-filled funnel-like vent, where the pumiceous turbidite emplaced. Distal facies of the deposit can be seen around the base of the peninsula. Around 15 km from the volcano, the distal facies (Oga pumice tuff) is a pyroclastic surge deposit with thicknesses of 1 to 1.5 m. Samples from both proximal and distal deposits were FT-dated and showed similar results (ca. 0.4 Ma).

Megata volcano

The Metaga volcano consists of three maars: Ichinomegata, Ninomegata, and Sannomegata. These maars are filled with water to form round ponds. The Ichinomegata maar is ca. 800 m in diameter and larger than the other two maars, both of which are ca. 500 m in diameter. The Ninomegata maar dissected the eastern inside slope of the Toga volcano, implying that the maar is younger than the Toga volcano (0.4 Ma). The formation ages of Ichinomagata and Sannomegata were determined with the stratigraphic relations to a widespread tephra (AT, or Aira-Tn tephra: a 25 ky tephra from the Aira caldera in southern Kyushu) and terrace deposits along with ^{14}C dating (Kitamura, 1990): Ichinomegata was formed during the period between 100 ka and 80 ka, and San-nomegata during the period between 24 ka and 20 ka. The formation age of Ninomegata is unknown because eruption products from Ninomegata have not been identified.

The eruption products from Ichinomegata have been well described. The products consist of lapilli tephra, ash tephra, and pumiceous lapilli tephra. The deposits occur as intercalated layers, ranging from several cm to 2 m in thickness. The ash and lapilli layers abundantly contain various types of lithic fragments of volcanic and plutonic rocks, including xenoliths of amphibolite and mantle-derived peridotite. Essential fragments consist of calc-alkaline andesite. From the sedimentary structures and aspects of pyroclasts, the tephras are considered to be surge and fall deposits from phreatomagmatic eruptions (Katsui, 1979).

Eruption products from Sannomegata dominantly consist of basaltic scoria, accompanying various types of accidental lithic fragments. The scoria deposit exhibits bedding and laminar structures. Both accidental and essential fragments are blocky. These characteristics imply that the scoriaceous layer was deposited from base surge (Kano *et al.*, 2011).

10-1. Petrology

Kano *et al.* (2002) and Aoki (1989) described the petrological features of pumice from the Toga volcano. The pumice clasts consist of glass, biotite, sanidine, quartz, plagioclase, opaque mineral, and rare amphibole. Sandy ash contains minor pyroxene crystals, which are not contained in the pumice clasts, implying that they were accidental fragments. The pumice clasts are alkali-rhyolite. Silica contents of the pumice clasts range from 71 to 74 wt%. They are rich in alkali element, *e.g.*, K_2O content ranging from 4.2 to 5.2 wt%.

Magmatic fragments ejected from the Megata volcano are basaltic scoria (Sannomegata), and andesitic and dacitic pumice (Ichinomegata). Pumice clasts from the Ichinomegata volcano are high-K andesite and dacite containing plagioclase, quartz, biotite, hornblende, augite, and opaque minerals as phenocrysts. Scoria clasts from Sannomegata are high-alumina basalt. Part of them is as magnesian as equilibrium with mantle peridotite (Yoshinaga and Nakagawa, 1999).

Abundant ultramafic (spinel lherzolite, hurzburgite, and websterite) and mafic xenoliths (hornblend gabbro and amphibolite) from the deep

Geologic Age		Geologic Unit		Lithology	Isotopic age
Neogene	Early Miocene	Daijima Formation		Conglomerate, Sandstone, silstone, and mudstone	20.1±0.8Ma (FT)
		Nomuragawa Formation	Tateyamazaki dacite	Dacitic pyroclastic rocks	21.4±0.8 Ma (FT)
			Honzan vent-filling deposits	Dacitic welded pyroclastic rocks, and volcanic breccia	
			Nomuragawa Dacite II	Dacitic pyroclastic rocks	
			Nomuragawa Basalt	Basaltic andesite lava and pyroclastic rocks	19.8±1.7, 20.2±0.8, 20.9±0.3 Ma (K-Ar)
			Nomuragwa Dacite I	Welded dacitic pyroclastic rocks	
			Nomuragwa Tuffaceous Conglomerate	Conglomerate, sandstone, and minor siltstone	20.9±0.3, 22.0±1.1, 21.8±0.6, 21.9±0.7 Ma (FT)
Paleogene	Oligocene				
	Late Eocene	Monzen Formation	Shinzan Rhyolite	Rhyolitic subaqueous lava and pyroclastic rocks	34.04±0.16 Ma (Ar-Ar) 34.06±0.78 Ma (K-Ar)
			Kenashiyama Andesite	Andesitic lava, tuffaceous conglomerate, and andesite lapilli tuff	31.4±0.8, 31.9±0.9 Ma (K-Ar)
			Nagasaki Dacite	Dacitic lappili tuff and tuff	27.1±1.3, 35.5±1.2 Ma (FT)
			Chorakuji basalt	Lavas and pyroclasitic rocks of alkali blasalt - trachyandesite and basalte - basaltic andesite	26.9±0.6, 29.9±0.7, 31.5±0.8 32.5±0.8, 34.3±0.9, 34.5±0.9 33.6±0.8 Ma (K-Ar)
			Ryugashima dacite	Trachytic - dacitic lavas, dacite pyroclastic rocks	27.1±1.3, 29.8±0.6 31.5±1.7 Ma (FT) 27.1±0.6 Ma (K-Ar)
			Butaijima Basalt	basalt - basaltic andesite lavas and pyroclastic rocks	31.1±0.7, 32.5±0.8, 32.8±0.8 33.8±1.1 Ma (K-Ar)
	Paleocene to Middle Eocene				
Late Cretaceous		Akashima Formation		Dacite welded pyroclastic rocks and volcanic breccia	71.53±0.64, 72.03±0.65 Ma (U-Pb) 49.3±0.2, 51.4±2.0, 53.4±1.4, 58.8±1.5 Ma (FT)

Figure 28. Volcanic stratigraphy at western Oga peninsula from Upper Cretaceous to Early Miocene, after Kano *et al.* (2011).

crust and the upper mantle occur in the pyroclastic deposit from Ichinomegata. Numerous previous studies were carried out on these mafic and ultramafic xenoliths to elucidate the mantle-crust structure, the mineralogical and geochemical nature beneath the arc, and the ascending velocity of the magma.

11. Neogene volcanics in the Oga peninsula

11-1. Introduction

The Neogene stratigraphy of the Oga peninsula has been extensively carried out since the beginning of the 20th century to establish the type section of the rear-arc region of northern Honshu, which is a petroleum-prospected region. After Fujioka (1959) established the excellent Neogene stratigraphy of the peninsula, numerous biostratigraphic studies were carried out to unravel a detailed chronology for sedimentary rocks. On the other hand, the Miocene volcanic rocks, the so-called "Green Tuff", had not been geologically studied until the 1990s, except for some FT dating studies. Since the hypothesis that the Green Tuff was related to the opening of the Sea of Japan has become accepted, the geology of Neogene volcanic rocks has been reexamined in detail (Fig. 28; Oguchi *et al.*, 1995; Kobayashi, 2004, 2008; Kano *et al.*, 2011).

11-2. Geology

There are three formations consisting of old volcanic rocks in the western Oga peninsula: the Late Cretaceous Akashima Formation, the Late Eocene Monzen Formation, and the Miocene Nomuragawa Formation (Kano *et al.*, 2011). The Akashima Formation, distributing around Nyudo-Zaki, which is the northwestern tip of the peninsula, is composed of dacitic pyroclastic rocks containing abundant basement granitic rock fragments. Ages recently determined by Zircon Pb-U are 71.53 ± 0.64 and 72.03 ± 0.65 Ma (Kano *et al.*, 2011). The Monzen Formation is broadly distributed over the western Oga peninsula. Volcanic products of the Monzen Formation exhibit a wide variety in composition from basalt to rhyolite. The volcanic sequence in the Monzen Formation has recently been well established (Oguchi *et al.*, 1995; Kobayashi, 2004, 2008; Kano *et al.*, 2011). The stratigraphic order from the bottom is Butaijima basalt, Ryugasima dacite, Chorakuji basalt (27 to 35 Ma, K-Ar), Nagasaki dacite, Kenashi-Yama andesite, and Shinzan rhyolite. At Kabuki-Iwa in the northeastern coast, Chorakuji basalt occurs as a pile of pillow lava and associated breccia. A number of K-Ar and FT dating for samples from all these members range from ca. 27 Ma to ca. 35 Ma. The Nomuragawa Formation consists of tuffceous sandstone, dacitic pyroclastic rocks, and basaltic andesite lava and pyroclastic rocks. The K-Ar age of the basaltic andesite is ca. 21 Ma (Kobayashi *et al.*, 2004).

Description of Field Trip Stops

Bandai volcano

Please see Figure 29 for the locations of the stops.

Stop (Bd-1): Panoramic view of Okinajima debris avalanche deposit

At the first stop of this field trip, we will show an excellent panoramic view of the Okinajima debris avalanche deposit dipping gently towards the west with many hummocky hills at the surface. We will also see the beautiful lake "Inawashiro" which might have been (at least partly) due to the damming up of the old Nippashi river by the Okinajima debris avalanche that had occurred 46 ka. The remnant wall of the amphitheater formed by this sector collapse is scarcely recognized, just like a drape of the Oh-Bandaisan cone.

Stop (Bd-2): The Bandai 1888 Eruption Memorial Museum

The Bandai 1888 Eruption Memorial Museum was built on the surface of the debris avalanche deposit of the AD 1888 eruption event. At this point, we will observe the well-preserved cutting of one of the hummocky hills in the main depositional area of the debris avalanche. We will easily find several features typical of the debris avalanche deposit, such as patchwork structure, jigsaw cracks in the lava blocks, and co-occurrence of block facies and matrix facies. We can enjoy an ordinary exhibition program of the Bandai 1888 Eruption Memorial Museum afterwards.

Stop (Bd-3): The amphitheater formed at AD 1888 sector collapse and outlook of the main deposition area of debris avalanche via avalanche valley

Stop Bd-3a: Way out of the ski rift. Stop 3a is located just at the connecting zone of the crater area with the avalanche valley. Scraping of the ground surface by friction of flowing debris is generally considered as the most promising cause for the forming of the avalanche valley (Nakamura, 1978; Moriya, 1988), but several studies have claimed that this type of box canyon must be the result of a stepwise collapse of the edifice (Yonechi, 1987; Sekiguchi *et al.*, 1997). We will also enjoy a beautiful view of the main depositional area (of the debris avalanche) with its resultant dammed-up lakes.

Stop Bd-3b: Akanuma. To the east, the cross section of the Kushigamine stratocone is well cropped out on the crater wall. We readily recognize that several massive lava flows with intercalating pyroclastics make up the Kushigamine edifice. We can also see the inside structure of the Akahaniyama, which is composed of stratified and oxidized (sulfurized) tephra layers. In the southern to the western part of the wall several fumaroles will be recognized. Talus due to the collapse of the wall that occurred in 1954 also rests near the fumarole-rich area.

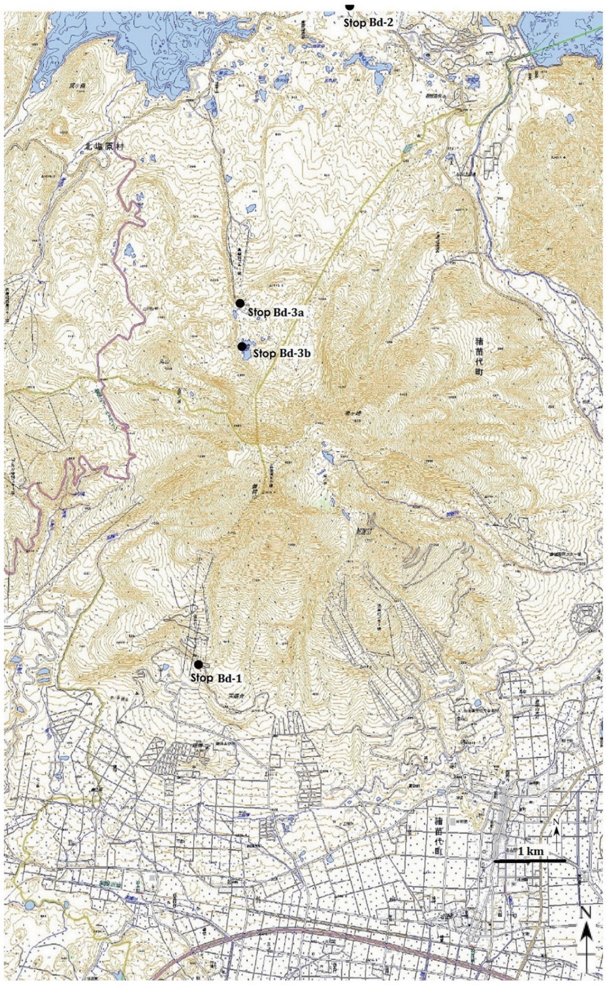

Figure 29. Locations of the observation points of Bandai volcano.

Azuma volcano

Please see Figure 30 for the locations of the stops.

Stop (Az-1): Trekking around the crater rim of the Azuma-Kofuji pyroclastic cone

Azuma-Kofuji is a cinder cone created about 6 ka, consisting of bread-crust bombs, agglutinate, and rootless lava (Fig. 13). This field trip will enjoy trekking along the trail around the crater rim of the Azuma-Kofuji.

Stop Az-1a: At the northern rim of the crater, we can find a variety of essential ejecta, such as scoria, pumice, and bread-crust bombs of andesitic to dacitic compositions. We will also get a view of the old amphitheater floor (Johdo-daira) with several small craters formed on it.

Stop Az-1b: At the eastern rim, the lava that flowed eastward from the Azuma-Kofuji crater may be seen. We can notice some surface micro-topographic structures, such as lava levee, lava wrinkles, and tongue-shaped fronts on each lobe of the lava flow.

Stop Az-1c: We will have a brief stop at the southeastern rim to look at an outcrop of the densely welded agglutinate composed of essential magmatic fragments such as scoriae, spatters, and driblets. This deposit was remobilized to flow to the southwest and formed clastogenic lava.

Stop (Az-2): Trail to the Oh-Ana crater near the northern rim of the Johdo-daira

Fifteen minutes by foot from the parking area, we will observe and have a close-up view of several gigantic bread-crust bombs with a maximum diameter ca. 6 m. This might be a sort of block and ash flow deposit ejected in the AD 1331 eruption.

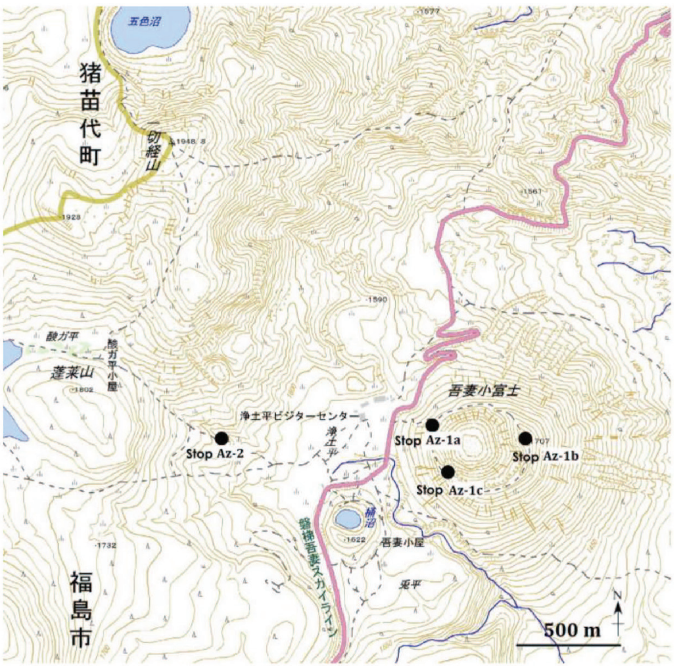

Figure 30. Locations of the observation points of Azuma

Zao volcano

Please see Figure 31 for the locations of the stops.

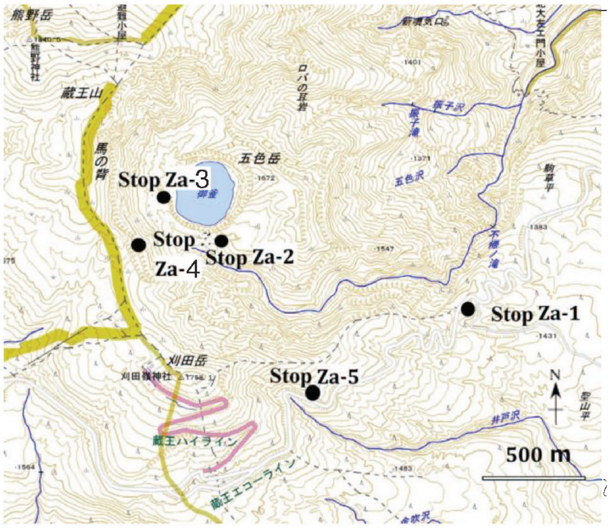

Figure 31. Locations of the observation points of Zao volcano.

Stop (Za-1): Tephra layers ca. past 30 ky activities

Look at the facies between proximal and distal of the most recent stage (ca. 30 ka ~ recent) of the Zao volcano (Figs. 15 and 16). Pyroclastic surge deposits of the Komakusadaira agglutinate are covered by tephra layers of Umanose agglutinate and Goshikidake pyroclastic activities. The contrasting feature of the deposit of each activity is visible in outcrops in this area.

Stop (Za-2): The Goshikidake pyroclastic cone

Three minutes by foot from the parking area, we can see the Goshikidake pyroclastic cone, formed by < ca. 2 ka activity (Fig. 15). It is still active. This cone consists mainly of successions of pyroclastic surge and associated pyroclastic fall deposits. Thicker agglutinate layers are sometimes observed. The Okama crater lake has been active since AD 1227. Before that, the crater was in just southwest of the Okama. The morphology of the former crater is preserved.

Stop (Za-3): The AD 1895 eruption products

The deposits of white-gray color draping the Goshikidake pyroclastic cone are of AD 1895 hydrothermal pyroclastic eruption deposits (Fig. 17). The eruption products consist mainly of hydrothermally altered ash with altered blocks, except for ash from 1984. The eruption deposits of

1895 are divided lithologically into six layers (1–6). Comparison of the document with the lithofacies of deposits shows that layers 1, 2, 3–4, and 5–6 were correlated respectively with eruption episodes of 15th February (episode 1), 19th February (episode 2), 22nd August (episode3), and 27th–28th September (episode 4).

Stop (Za-4): The calc-alkaline basaltic lava flows

When the weather is fine, we can enjoy the optional view of calc-alkaline basaltic lava flows widely exposing the west cliff of the Umanose caldera wall (Fig. 32). The lava is about 20 m thick. The platy joint is dominated in the lower part, while the columnar joint is obvious in the middle part.

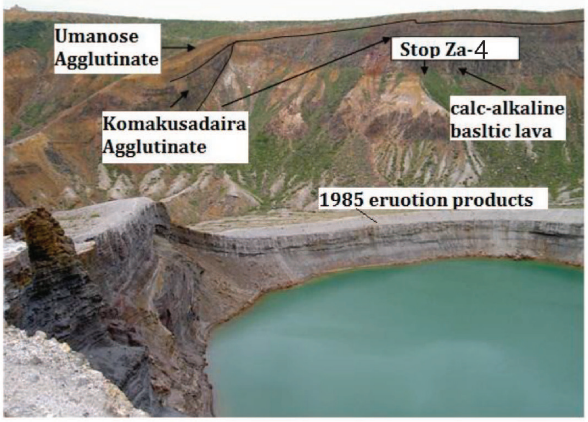

Figure 32. A photograph of eruption products observed in west wall of the Umanose caldera.

Stop (Za-5): Various facies of pyroclastic density currents of the Komakusadaira activity

The pyroclastic density current deposits of 30~1.8 ka activity can be observed. The pyroclastics show five facies: scoriaceous tuff, lapilli tuff, agglutinate, volcanic breccia, and tuff breccia. The scoriaceous tuff facies is characterized by black to dark gray scoriaceous ash and crystal fragments. The lapilli tuff facies is characterized by andesitic lapillus with a minor amount of black to dark gray scoriaceous ash. The agglutinate is composed mainly of scoria fragments (including spatter) with minor amounts of finer ones or ash matrix. They are well or poorly sorted. The volcanic breccia facies is poorly sorted, clast-supported, and characterized by abundant lithics in the matrix of altered blown ash. The tuff breccia facies is characterized by abundant lithics in white to yellow clay matrix. The main components of each episode, except for episodes 2–4, show scoriaceous tuff facies, whereas those of episodes 2–4 show agglutinate facies. The other three facies are sometimes observed intercalating into the pyroclastic succession.

Iwate volcano

Please see Figure 33 for the locations of the stops.

Stop (Iw-1): Yake-bashiri lava flow at AD 1732

We will observe the Yake-bashiri lava flow and the craters on the northeast flank of the Higashi-Iwate volcano. The craters were formed by the 1732 activity, the most recent magmatic activity of the Iwate volcano. The Yake-bashiri lava flow traveled down the NE flank. We will observe the surface of the a'a type lava. If the weather is fine, we will be able to see the craters for the lava flow arranging in a linear line.

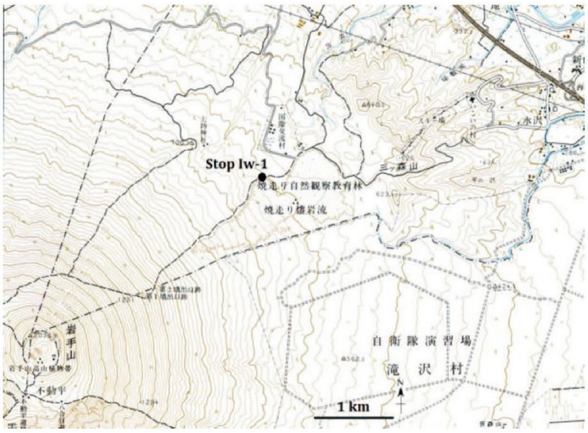

Figure 33. Locations of the observation points of Iwate volcano.

Hachimantai, Akita Yakeyama, and Tazawako

Please see Figures 34 and 35 for the locations of the stops.

Stop (Ha-1): Hydrothermal eruption craters on the Hachimantai summit plateau

More than 20 hydrothermal craters are situated on the summit plateau of Hachimantai (Fig. 25). You can access these craters easily, by driving a car through a wide road to the park near the summit and walking just a few minutes from the park. The car park is located just above the crown of the old landslide that triggered the hydrothermal eruption. The sightseeing trail passes through some of the craters. Presently, hydrothermal activity is not active on the crater area, where forest, grass, and bogs cover the ground. The craters are filled with water. The biggest pond, Hachiman-Numa, consists

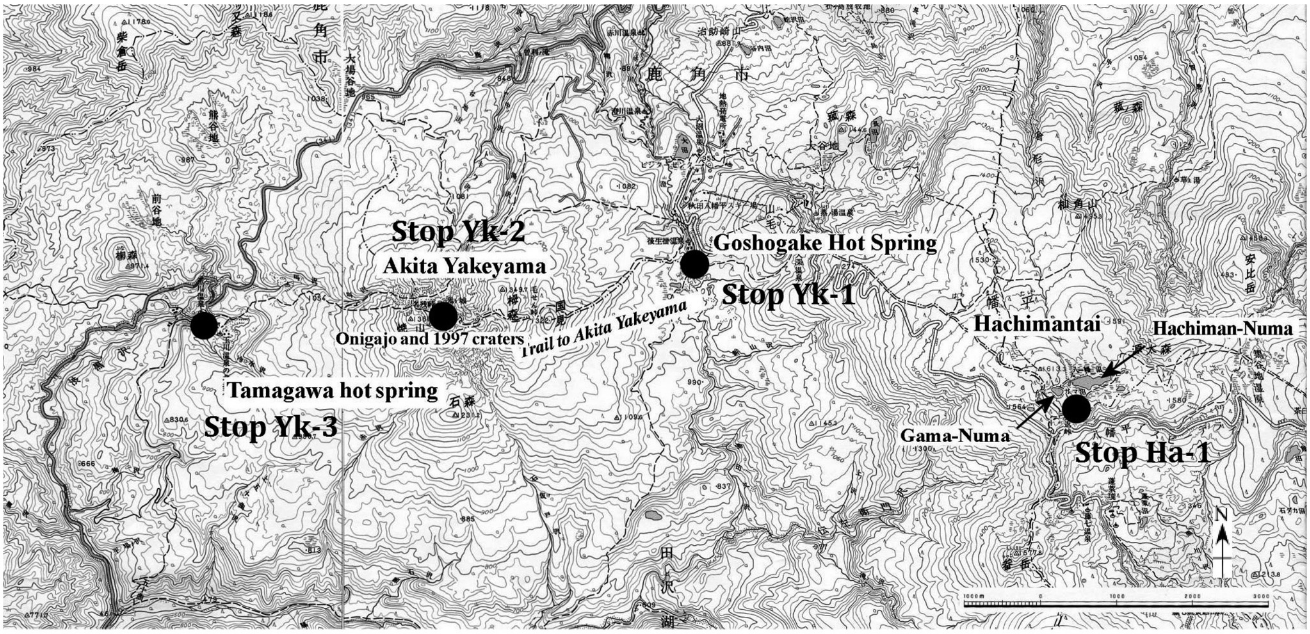

Figure 34. Locations of the observation points of Hachimantai and Akita-Yakeyama area.

of long-connected hydrothermal craters. The gourd-shape crater, Gama-Numa, consists of coalesced two craters. You can find many other craters along the trail.

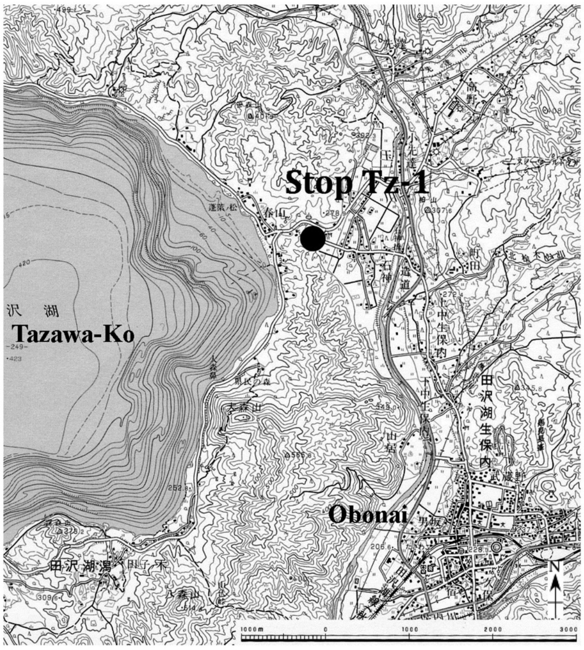

Figure 35. Locations of the observation point of lake side of Tazawa-ko.

Stop (Yk-1): Goshogake Hot Spring - Trail to Akita Yakeyama

The area around the old-Japanese style hotel of the Goshogake hot spring is an active geothermal area, where you can see fumarole, sulfur deposits, mud pods, hot springs, warm ground, and steaming pools. The area is famous for "mud volcanoes"—small muddy cones formed by the intermittent ejection of boiling mud. As the area is a famous sightseeing spot, many tourists visit here from spring to autumn. This place is also the base of the tramping trail to Akita Yakeyama.

The trail from the Goshogake hot spring to the summit of Akita Yakeyama goes through a forest of beech trees and Sakhalin fir. It takes about an hour and a half to get to the summit area. The trail is mostly covered by mud, boulders, and leaves, but young volcanic ash layers can be occasionally seen in small exposures along the trail (Fig. 36). The exposures may contain phreatic and phreatomagmatic ash fall layers from Akita Yakeyama and a widespread tephra from the Towada caldera from AD 915.

Stop (Yk-2): Akita Yakeyama Summit Crater

In the summit area, there is a central crater 1 km wide. A dacitic dome (Onigajo dome) is located at the center of the central crater. Passing through the summit hut, the trail accesses the top of the Onigajo dome. Viewing north from the top of the dome, you will see that the dome is dissected by a crater 100 m wide, the Karanuma crater. The gray ground in the southeastern half of the crater bottom is the mudflow deposit of the 1997 hydrothermal eruption (Figs. 26 and 37). The mudflow effused from the southeastern end of the crater bottom. The

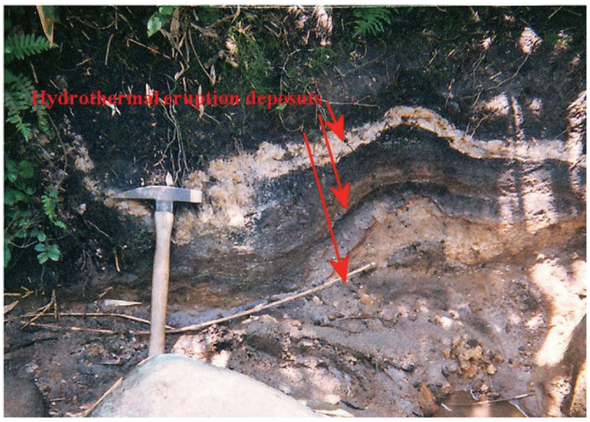

Figure 36. Hydrothermal eruption deposits from Akita Yakeyama, intercalating with black soil layers at an small outcrop along the trail.

other crater of the 1997 eruption is located on the southeastern rim of the crater, or at the tip of the crescent-shaped lava dome. At the crater, explosive discrete eruptions occurred, and fallen mud and blocks were thickly deposited around the crater.

At the western bottom of the central crater, there is a crater lake with hot acid water. Many fumaroles, hot springs, mud pods, and sulfur deposits are distributed around the lake, and ground temperatures are always high. This vigorous geothermal area extends beyond the crater wall. In the head valley of a radial gully (Sakebizawa), geothermal activity is similarly intense.

Stop (Yk-3): Tamagawa Hot Spring

At the western base of the stratocone, there is also a geothermally active area with a Japanese-traditional Onsen hotel. Fumaroles, mud pods, and hot springs are distributed over the field, similar to other geothermal fields. What one should see in this field is a hot spring called Obuki. Most of the acid fluid souring the surface on the volcanoes are sulfuric, or steam-heated-type fluid. On the other hand, Obuki is a sulfuric-chloride acid hot spring, which is considered the least differentiated fluid from magmatic water. The Tamagawa hot spring is also famous for the occurrence of rare mineral hokutolite, which is a Pb-bearing sulfate mineral. As hokutolite is designated as a Special National Treasure,

Figure 37. Craters and products of the 1997 hydrothermal eruption at Akita Yakeyama. Viewed from northern rim of Karanuma crater.

collecting hokutolite is strictly prohibited here.

Stop (Tz-1): Pumiceous deposit from Tazawa-Ko

At a roadside outcrop near Tazawa-Ko, a thick massive pumiceous deposit is exposed. In spite of the good accessibility to the outcrop, the origin of the deposit (both source and transport mechanism) has not been well investigated and is still controversial. Recent studies demonstrate that this deposit was derived from the Tazawako caldera 1.8–1.4 Ma. The idea that Tazawa-Ko is an old caldera is quite new. The deposit characteristically contains large quartz crystals, but this feature is common in ignimbrites in Sengan volcanic field.

Oga Peninsula

Please see Figure 38 for the locations of the stops.

Stop (Og-1): Hachibo-Dai

From the observation deck of Hachibo-Dai, the Toga volcano and Megata maar volcanoes can be seen except for Sannomegata, which is hidden behind a hump near the coast. Although

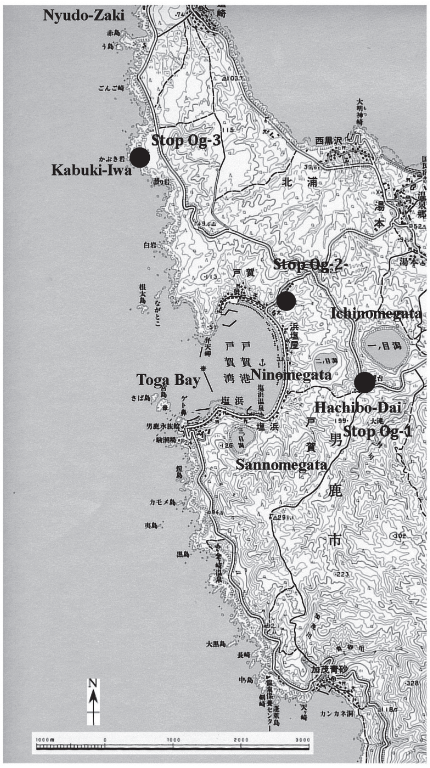

Figure 36. Hydrothermal eruption deposits from Akita Yakeyama, intercalating with black soil layers at an small outcrop along the trail.

Ichinomegata is very famous for the occurrence of peridotite xenoliths, collecting the rocks has been strictly prohibited and access to the lakeside is closed.

Stop (Og-2): Toga Pumice

Proximal exposure of volcanic products from the Toga volcano is very limited. In the northeastern inside slope of the volcano, a thick pumiceous deposit is exposed in a small gorge. These stratified and partly cross bedded layers of pumice, ash, and breccia were extensively described by Kano *et al.* (2002). The paleocurrents are bidirectional, implying that the pyroclastic materials slid back inside the crater during the eruption.

Stop (Og-3): Kabuki-Iwa

In Japan, there are many outcrops of pillow lava, where you can observe the cross sections of lava structures. In this place, however, you can observe a excellent three-dimensional structure of old Eocene pillow lava flows (Fig. 39). There are various kinds of lobe structure, such as lava wrinkles, multiple crusts, and extensional cracks. Near this point, the basalt occurs as a'a and pahoehoe lavas, implying that the volcanic activity occurred at a transitional zone between subaerial and subaqueous environments. Zeolite filling vesicles forms amygdules.

Acknowledgments

Review comments fom Prof. A. Toramaru and Dr. M. Yoshimoto were very helpful in revising the manuscript.

References

Anzai, T. (1961) A Mysterious Crater Lake, Okama of Zao. Yamagata Geological Research Laboratory, 224p. (in Japanese)

Aoki, K. (1989) Mugearite, trachyandesite, trachyte, and alkali basalt. In: Kushiro, I. *et al.* (Eds.), Japanese Igneous Rocks. Iwanami, 95-103. (in Japanese)

Ban, M., (2007) Magma feeding system of the andesitic active volcanoes in central and southern parts of NE Japan. In: Ida, Y. (Eds.), Research Report of Grant-in-Aid for Scientific Research on Priority Areas: Dynamics of Volcanic Eruption, **5**, 367-375.

Ban, M., Oba, Y., Ishikawa, K. and Takaoka, N. (1992) K-Ar dating of Mutu-Hiuchidake, Osoreyama, Nanashigure, and Aoso volcanoes of the Aoso-Osore volcanic zone - The formation of the present volcanic zonation of the Northeast Japan arc. Jour. Mineral. Petrol. Econ. Geol., **87**, 39-49 (in Japanese with English abstract)

Ban, M., Sagawa, H., Miura, K. and Hirotani, S. (2008) Evidence for short-lived stratified magma chamber: petrology of Z-To tephra layer (~ 5.8 ka) at Zao volcano, NE Japan. In: Zellmer, G. and Annen, C. (Eds.), Dynamics of Crustal Magma Transfer, Storage, and Differentiation Integrating Geochemical and Geophysical Constraints. Geol. Soc. London, Special Publication, **304**, 149–168.

Ban, M., Sagawa, H., Miura, K. and Tanaka, Y. (2005) Volcanic hazard map of Mt. Zao. Earth Monthly, **27**, 317–320. (in Japanese)

Centennial Project Body of the Bandai Eruption (1988) Centennial memorial publication of the Bandai eruption. Committee of Centennial Memorial Publication of the Bandai Eruption, Aizu-Wakamatsu, Japan. 189 p. (in Japanese)

Chough, S.K. and Sohn, Y.K. (1990). Depositional mechanisms and sequences of base surges, Songaksan tuff ring, Cheju Island, Korea. Sedimentology, **37**, 1115–1135.

Cole, P.D. (1991) Migration direction of sand-wave structures in pyroclastic surge deposits: implications for depositional processes. Geology, **19**, 1108–1111.

Doi, N. (2000) Geology of Iwate volcano. Archaeological Researches in Takizawa, 32, The Board of education in Takizawa Iwate Prefecture. 234p.

Doi, N. (2010) Phreatic explosions caused by the large-scale landslide at Kurikoma and Hachimantai volcanoes. Abstr. Fall Meeting Volcanol. Soc. Japan, 15. (in Japanese)

Frazzetta, G., La Volpe, L. and Sheridan, M.F. (1983) Evolution of the Fossa Cone, Vulcano. In: Sheridan, M.F. and Barberi, F. (Eds.), Explosive Volcanism. Jour. Volcanol. Geotherm. Res., **17**, 329–360.

Fujinawa, A. and Kamoshida, T. (1999) Azuma volcano. In: Takahashi, M. and Kobayashi, T. (Eds.), Volcanoes in the Tohoku Region: Field Guide of Japanese Volcano 4. Tsukijishokan, Tokyo, 89–104. (in Japanese)

Fujinawa, A., Ban, M., Ohba, T., Kontani, K. and Miura, K. (2008) Characterization of low temperature pyroclastic surges that occurred in the northeastern Japan arc during the late 19th century. Jour. Volcanol. Geotherm. Res., **178**, 113–130.

Fujinawa, A., Iwasaki M.,, Honda,. K., Nagao, A., Wachi, T. and Hayashi, S. (2004) History in the Post-caldera Stage of Akita-Komagatake Volcano, Northeastern Japan Arc: Correlation between Eruptives Constituting Volcanic Edifices and Air-fall Tephra Layers. Bull. Volcanol. Soc. Japan, **49**, 333-354. (in Japanese with English abstract)

Fujioka K. (1959) Toga and Funakawa. 1:50000 Geological Map. Geol. Surv. Japan, 61p. (in Japanese with English abstract)

Hoblitt, R.P., Miller, D.C. and Vallance, J.E. (1981) Origin and stratigraphy of the deposits produced by the May 18 directed blast. In: Lipman, P.W. and Mullineaux, D.R. (Eds.), The 1980 Eruptions of Mount St. Helens, Washington. U.S. Geol. Surv. Prof. Pap., **1250**, 401–419.

Huang, Z., Zhao, D. and Wang, L. (2011) Seismic heterogeneity and anisotropy of the Honshu arc from the Japan Trench to the Japan Sea. Geophys. Jour. Int., **184**, 1428-1444.

Ichimura, T. (1951) Geological investigations on the Zao volcanoes. I. Goshiki-dake, a central cone of the Zao proper. Bull. Earthq. Res. Inst., **29**, 327-339.

Ichimura, T. (1960) Geological investigations on the Zao volcanoes, V. Kumano volcano. Bull. Earthq. Res. Inst., **38**, 255-290.

Imura, R. (1999) Zao volcano. In: Takahashi, M. and Kobayashi, T. (Eds.), Volcanoes in the Tohoku Region: Field Guide of Japanese Volcano 4. Tsukijishokan, Tokyo, 70–88. (in Japanese)

Ishikawa, K., Yoshida, T. and Aoki, K. (1982) Geochemistry of Iwate volcano. Res. Rep. Lab. Nuc. Sci. Tohoku Univ., **15**, 257-264. (in Japanese)

Itoh, J. (1998) The eruption history of Iwate volcano in the Edo period, based on the historical documents. Bull. Volcanol. Soc. Japan, **43**, 467-481. (in Japanese with English abs)

Itoh, J. (1999) Eruption sequence and ^{14}C age of phreatic eruptions occurred at West-Iwate volcano in historic age. Bull. Volcanol. Soc. Japan, **44**, 261-266. (in Japanese with English abs)

Kano, K., Ohguchi, T., Hayashi, S. and Yanai, K. (2007) Tazawako caldera and its eruption products, Abstr. Annual Meeting Geol. Soc. Japan, 70. (in Japanese)

Kano, K., Ohguchi, T., Hayashi, S., Uto, K. and Danhara, T. (1999) Toga volcano: an alkali-rhyolite tuff-ring in the western end of Oga peninsula, NE Japan. Abstr. Fall Meeting of Volcanol. Soc. Japan, 100. (in Japanese)

Kano, K., Ohguchi, T., Hayashi, S., Uto, K. and Danhara, T. (2002) Toga volcano: an alkali-rhyolite tuff-ring in the western end of Oga peninsula, NE Japan. Bull. Volcanol. Soc. Japan, **47**, 373-396. (in Japanese with English abstract)

Kano, K., Ohguchi, T., Yanagisawa, Y., Awata, Y., Kobayashi, N., Sato, Y., Hayashi, S., Kitazoto, H., Ogasawara, K. and Komazawa, M. (2011) Geology of the Toga and Funakawa District 2nd Edition. Quadrangle series, 1:50000, Geol. Surv. Japan, AIST, 127p. (in Japanese with English abstract)

Kamoshida, T. (1991) Ages of caldera collapse and subsequent formation of Azuma-kofuji post caldera cone, Higashi-Azuma volcano: Estimation based on tephra stratigraphy. Abstr. of Volcanol. Soc. Japan Session in Annual Meeting of JpGU, 15. (in Japanese)

Katsui, Y. (1979) Genesis of calc-alkalic andesites from Oshima Oshima and Ichinomegata volcanoes, north Japan. Jour. Fac. Sci., Hokkaido Univ.. Ser. *IV*, Geol. Mineral., 19, 157-168.

Kawano, Y. and Aoki, K. (1959) Petrology of Hachimantai and surrounding volcanoes, northeastern Japan. Sci. Rep. Tohoku Univ., Ser. *III*, 6, 409-429.

Kawano, Y., Yagi, K. and Aoki, K. (1961) Petrography and petrochemistry of the volcanic rocks of Quaternary volcanoes of northeastern Japan. Sci. Rep. Tohoku Univ., Ser. *III*, 7, 1-46.

Kimura, J. and Yoshida, T. (2006) Contributions of slab fluid, mantle wedge and crust to the origin of Quaternary lavas in the NE Japan arc. Jour. Petrol. **47**, 2185–2232.

Kimbara, K. (1987) Hydrothermal rock alteration in the southern part of Hachimantai geothermal area, northeast Japan. Rep. Geol. Surv. Japan, 266. 211-221. (in Japanese with English Abstract)

Kitamura, S. (1990) Formation age of Megata volcano, Oga peninsula, Ann. Tohoku Geogr. Assoc., **42**, 161-167. (in Japanese)

Kneller, B.C. and Branney, M.J. (1995). Sustained high-density turbidity currents and the deposition of thick massive sands. Sedimentology, **42**, 607–616.

Kobayashi, N., Kano, K. and Ohguchi, T. (2004) The Nomuragawa Formation: proposal for a new stratigraphic unit in the west Oga Peninsula, NE Japan. Jour. Japanese Assoc. Petroleum Technologists, **69**, 374–384. (in Japanese with

English Abstract)

Kobayashi, N, Ohguchi, T. and Kano, K. (2008) Stratigraphic revision of the Monzen Formation, Oga Peninsula, NE Japan. Bull. Geol. Surv, Japan, 59, 211-224. (in Japanese with English Abstract)

Kuno, H. (1962) Japan, Taiwan and Marianas. Catalog of Active Volcanoes of the World and Solfatara Fields, Rome: IAVCEI, **11**, 1-332.

Kuno, H. (1966) Lateral variation of basalt magma type across continental margins and island arcs. Bull. Volcanol., **29**, 195–222.

Mimura, K. and Nakamura, Y. (1997) Geological history and petrography of Bandai volcano. Research group for the origin of debris avalanche research by the special coordination funds for promoting science and technology, Science and Technology Agency, Japan, 103-120.

Miura, K., Ban, M. and Yagi, H. (2008) The tephra layers distributed around the eastern foot of the Zao volcano - Ages and volumes of the Za-To 1 to 4 tephras -. Bull. Volcanol. Soc. Japan,. **53**, 151-157.

Miura, K., Ban, M., Ohba, T. and Fujinawa, A. (2012) Sequence of the 1895 eruption of the Zao volcano, Tohoku Japan. Jour. Volcanol. Geotherm. Res., **247-248**, 139-157.

Moriya, I. (1983) Geomorphology of Japanese volcanoes. Tokyo Univ. Press, 135p. (in Japanese)

Moriya, I. (1988) Geomorphological development of Bandai volcano. Jour. Geogr., **97**, 293-300. (in Japanese with English abstract)

Murayama, I. (1973) Volcanic activity and topography, Taimeido, 308p. (in Japanese)

Nakagawa, M. (1987) Geology of Iwate volcano, NE Japan. Jour. Mineral. Petrol. Econ. Geol., **82**, 132-150. (in Japanese with English abstract)

Nakagawa, M. (1994) Deep level crystallization of arc basalts: polybaric crystallization of island arc tholeiitic basalts from Iwate volcano. Abstr.act Annual Meeting of JpGU, B12-1. (in Japanese)

Nakagawa, M. and Togari, H. (1999) Petrologic aspect on Iwate volcano: Petrologic features of recent magma system and volcanic activity of Iwate volcano. Earth Monthly, **21**, 264–268. (in Japanese)

Nakagawa, M., Shimotori, H. and Yoshida, T. (1988) Across-arc compositional variation of the Quaternary basaltic rocks from the Northeast Japan arc. Jour. Mineral. Petrol. Econ. Geol., **83**, 9–25. (in Japanese with English abstract)

Nakajima, J., Matsuzawa, T., Hasegawa, A. and Zhao, D. (2001) Three-dimensional structure of Vp, Vs and Vp/Vs beneath northeastern Japan arc: Implications for arc magmatism and fluids. Jour. Geophys. Res., **106**, 21843–21857.

Nakamura, Y. (1978) Geology and petrology of Bandai and Nekoma volcanoes. Sci. Rep. Tohoku Univ., Ser. *III*, 14, 67-119.

Nakamura, Y. and Aoki, K. (1980) Bandai volcano. Earth Monthly, **2**, 430–434. (in Japanese)

Nakamura, Y. and Glicken, H. (1988) Blast and debris-avalanche deposits of the 1888 eruption, Bandai volcano. Jour. Geogr., **97**, 67–74. (in Japanese with English abstract)

Nakamura, Y. and Glicken, H. (1997) Debris avalanche deposits of the 1888 eruption, Bandai volcano. Research group for the origin of debris avalanche research by the special coordination funds for promoting science and technology Science and Technology Agency, Japan, 135-147.

NEDO (1991a) Geological and geothermal survey maps of Azuma distric, 80p.

NEDO (1991b) National geothermal resource survey in 1990 - survey on regional geothermal fluid system: atlas of geothermal survey on Akitakoma district, 119p.

Nemeth, K., Martin, U. and Harangi, Sz. (2001) Miocene phreatomagmatic volcanism at Tihany (Pannonian Basin, Hungary). Jour. Volcanol. Geotherm. Res., **111**, 111–135.

Nishimura, T., Nakamichi, H., Tanaka, S., Sato, M., Kobayashi, T., Ueki, S., Hamaguchi, H., Ohtake, M. and Sato, H. (2000) Source process of very long period seismic events associated with The 1998 activity of Iwate volcano, northeastern Japan. Jour. Geophys. Res., **105**, 19135-19147.

Oba, Y. and Konta, T. (1989) Geology and petrology of central Zao volcano, Yamagata prefecture. Bull. Yamagata Univ. Natural Sci., **12**, 199–210. (in Japanese with English abstract)

Oguchi, T., Hayashi, S., Kobayashi, N., Itaya, T. and Yoshida, T. (1995) K-Ar dating unravels the volcanic history of the Kuguriiawa Lava and Kamo Lava members, Oligoxene Monzen Formation, Ogapeninsula, NE Japan. Mem, Geol. Soc. Japan, **44**, 39-54. (in Japanese with English Abstract)

Ohba, T. (1993) Geology and petrology of Akita Yakeyama volcano 2 : evolution of magmatic composition. Jour. Mineral. Petrol. Econ. Geol. Japan, **88**, 1-19. (in Japanese with English abstract)

Ohba, T. and Umeda, K. (1999) Geology of Hachimantai volcanic field and temporal-spatial variation of the magma compositions. Jour. Mineral. Petrol. Econ. Geol., **94**, 187-202. (in Japanese with English abstract)

Ohba, T., Hayashi, S., and Umeda, K. (2003) K-Ar ages of volcanic rocks from northern vicinity of Matsukawa geothermal field, Iwate Prefecture. Bull. Volcanol. Soc. Japan, **48**, 367-374. (in Japanese with English abstract)

Ohba T., Kimura, Y. and Fujimaki, H. (2007a) High magnesian-andesite produced by two-stage magma mixing: a case study from Hachimantai, norhtern Honshu, Japan. Jour. Petrol., **48**. 627-645.

Ohba, T., Taniguchi, H., Miyamoto, T., Hayashi. S. and Hasenaka, T. (2007b) Mud plumbing system of an isolated phreatic eruption at Akita Yakeyama volcano, northern Honshu, Japan. Jour. Volcanol. Geotherm. Res., **161**, 35-46.

Ohba, T., Matsuoka, K., Kimura, Y., Ishikawa, H. and Fujimaki, H. (2009) Deep crystallization differentiation of arc tholeiite basalt magmas from northern Honshu arc, Japan. Jour. Petrol., **50**, 1025-1046.

Omori, F. (1893) Report on the eruption of Azuma volcano. Bull. Earthquake Investigation Committee, **1**, 60-62. (in Japanese)

Onuma, K. (1962) Petrology and petrochemistry of the rocks from Iwate volcano, northeastern Japan. Jour. Japan Assoc. Mineral. Petrol. Econ. Geol., **47**, 192-204.

Sakayori, A. (1991) Magmatic evolution of Zao volcano, Northeast Japan. Bull. Volcanol. Soc. Japan, **36**, 79–92. (in Japanese with English abstract)

Sakayori, A. (1992) Geology and petrology of Zao volcano. Jour. Mineral. Petrol. Econ. Geol., **87**, 433–444. (in Japanese with English abstract)

Sakuyama. M. and Nesbitt, R.W. (1986) Geochemistry of the Quaternary volcanic rocks of the Northeast Japan arc. Jour. Volcanol. Geotherm. Res., **29**, 413–450.

Sekiguchi, T., Haraguchi, K. and Iwahashi, J. (1997) Topographical configuration resulting from the 1888 eruption of Bandai volcano. Research group for the origin of debris avalanche research by the special coordination funds for promoting science and technology Science and Technology Agency, Japan. 155-165.

Sekiya, S. and Kikuchi, Y. (1888) Investigation report of Bandai-san. Official report, Sepember 27, 1888. (in Japanese)

Sekiya, S. and Kikuchi, Y. (1890) The eruption of Bandai-san. Tokyo Imp. Univ. Coll. Sci. Jour. **3**, 91–171.

Sendai District Meteorological Observatory (2013a) Volcanic activity of Azuma volcano, Jan 2013. In: Monthy volcanic activity report. http://www.seisvol.kishou.go.jp/tokyo/STOCK/monthly_v-act_doc/sendai/13m01/213_13m01.pdf

Sendai District Meteorological Observatory (2013b) Volcanic activity of Iwate volcano, Jan 2013. In: Monthy volcanic activity report. http://www.seisvol.kishou.go.jp/tokyo/STOCK/monthly_v-act_doc/sendai/13m01/207_13m01.pdf

Shigeno, H. and Abe, K. (1987) Conceptual hydrothermal system model for the Sengan area based on geochemistry of hot springs and fumaroles. Rep. Geol. Surv. Japan, 266. 251-283. (in Japanese with English Abstract)

Sohn, Y.K. and Chough, S.K. (1989) Depositional processes of the Suwolbong tuff ring, Cheju Island (Korea). Sedimentology, **36**, 837–855.

Suto, S. (1984) Paleomagnetic study and K-Ar age of volcanic rocks from Kayo-dake, Akita-prefecture, Northeast Japan. Bull. Volcanol. Soc. Japan, **29**, 112-114.

Suto, S. (1992) Explanatory text of the geological map of the central part of the Sengan Geothermal Area, scale 1:50,000. Miscellaneous Map Sereis (21-5), Geol. Surv. Japan, 73p. (in Japanese with English abstract).

Suto, S. and Mukoyama, S. (1987) Volcanic history at northern part of the Sengan geothermal area, northeast Japan, on the basis of paleomagnetic study. Rep. Geol. Surv. Japan, **266**. 143-158. (in Japanese with English Abstract)

Suto, S., Uto, K. and Uchiumi, S. (1990) K-Ar ages of the Nyuto Takakura volcanic products, southern part of the Sengan geothermal area, northeast Japan. Bull. Geol. Surv. Japan, **41**, 395-404.

Takahashi, T., Hirahara, Y., Miyazaki, T., Senda, R., Chang, Q., Kimura, J-I. and Tatsumi, Y. (2013) Primary magmas at the volcanic front of the NE Japan arc: coeval eruption of crustal low-K tholeiitic and mantle-derived medium-K calc-alkaline basalts at Azumavolcano. Jour. Petrol., **54**, 103-148.

Takaoka, N., Konno, K., Oba, Y., and Konta, T. (1989) K–Ar datings of lavas from Zao volcano, north-eastern Japan. Jour. Geol. Soc. Japan, **95**,

157–170. (in Japanese with English abstract)
Takashima, I. and Honda S., (1985) Issues on thermoluminescence dating for volcanic and altered rocks. Chinetsu, **22**, 215-223
Takebe, Y. and Ban, M. (2011) Temporal change of geologic features in the pyroclastic surge dominated deposits of the Komakusadaira pyroclastics in Zao volcano, NE Japan. International Journal of Geology, **5**, 1-13.
Tamura, Y., Tatsumi, Y., Y., Zhao, D., Kido, Y. and Shukuno, H. (2002) Hot fingers in the mantle wedge: New insights into magma genesis in subduction zones. Earth Planet. Sci. Lett., **197**. 105-116.
Tanaka, S., Hamaguchi, H., Ueki, S., Sato, M. and Nakamichi, H. (2002) Migration of seismic activity during the 1998 volcanic unrest at Iwate volcano, northeastern Japan, with reference to P and S wave velocity anomaly and crustal deformation. Jour. Volcanol. Geotherm. Res., **113**, 399-414.
Tanaka, K., Mimura, K., Endo, H. and Inokuchi, T. (1997) Slip surface and borings of catastrophic rockslide avalanche at Bandai volcano in 1888. Research group for the origin of debris avalanche research by the special coordination funds for promoting science and technology Science and Technology Agency, Japan, 81-92.
Tatsumi, Y. and Eggins, S. (1995) Subduction zone magmatism. Blackwell, Oxford, 211p.
Tatsumi, Y., Sakuyama, M., Fukuyama, H. and Kushiro, I. (1983) Generation of arc magmas and thermal structure of the mantle wedge in subduction zones. Jour. Geophys. Res., **88**, 5815–5825.
Tatsumi, Y., Takahashi, T., Hirahara, Y., Chang, Q., Miyazaki, T., Kimura, J.-I., Ban, M., and Sakayori A. (2008) New Insights into andesite genesis: The role of mantle-derived calc-alkalic and crust-derived tholeiitic melts in magma differentiation beneath Zao Volcano, NE Japan. Journal of Petrology, **49**, 1971-2008.
Tiba, T. (1961) Petrology of Zao volcano. Jour. Japan Assoc. Mineral. Petrol. Econ. Geol., **46**, 74–81. (in Japanese with English abstract)
Togari, H. and Nakagawa, M. (1998) Petrology of 1732 eruption products of Iwate volcano. Abstr. Fall Meeting of Volcanol. Soc. Japan, 11. (in Japanese)
Tsutsui, M., and Ito, H. (2002) Tephrochronological study of Akita-Yakeyama volcano -their origin, properties and eruptive age. Abstr. Fall Meeting of the Volcanol. Soc. Japan, 49. (in Japanese)
Uemura, F. (1987) Geological structure and geotectonic history of the Sengan geothermal area, Rep. Geol. Surv. Japan, 266, 25-41.
Umeda, K., Hayashi, S., Ban, M., Sasaki, M., Ohba, T., Akaishi, K. (1999) Sequence of the volcanism and tectonics during the last 2.0 million years along the volcanic front in Tohoku district, NE Japan. Bull. Volcanol. Soc. Japan, **44**, 233-249. (in Japanese with English abstract)
Wachi, T., Chiba, T., Yoshida, K., Doi, N. and Hayashi, S. (2002) Discovery of the Holocene tephra sourced from the Hachimantai volcano. Abstr. Annual Meeting of JpGU. V032-P005.
Waitt, R.B. (1981) Devastating pyroclastic density flow and attendant air fall of May 18 — stratigraphy and sedimentology of deposits. In: Lipman, P.W. and Mullineaux, D.R. (Eds.), The 1980 Eruptions of Mount St. Helens, Washington. U.S. Geol. Surv. Prof. Pap., **1250**, 439–458.
Wang, Z. and Zhao, D. (2005) Seismic imaging of the entire arc of Tohoku and Hokkaido in Japan using P-wave, S-wave and sP depth-phase data. Phys. Earth Planet. Interiors, **152**, 144-162.
Yamada, N. (1988) Eruption of Bandaisan and Mudflow at Nagasegawa River. Bunkashobou-Hakubunsha press, Japan. 249p. (in Japanese)
Yamamoto, T. (2005) Eruptive history of Azuma volcano, NE Japan, during last 7,000 years: Stratigraphy and magma plumbing system of the Azuma Jododaira products. Jour. Geol. Soc. Japan, **111**, 94-110. (in Japanese with English abstract)
Yamamoto, T. and Suto, S. (1996) Eruptive history of Bandai volcano, NE Japan, based on tephrostratigraphy. Bull. Geol. Surv. Japan, **47**, 335-359. (in Japanese with English abstract)
Yamamoto, T., Nakamura, Y. and Glicken, H. (1999) Pyroclastic density current from the 1888 phreatic eruption of Bandai volcano, NE Japan. Jour. Volcanol. Geotherm. Res. **90**, 191–207.
Yamamoto, T., Yoshioka, T., Makino, M. and Sumita, T. (2005) Geology of the Kitakata district.Quadrangle series, 1:50,000. Geological Survey of Japan, AIST, 63p (in Japanese with English abstract 5p.).
Yokoyama, M. (1893) Eruption of Mt. Azuma. Jour. Geography, **5**, 533-541, 583-596. (in Japanese)
Yonechi, F. (1987) A new hypothesis on the collapse of Bandai-san volcano in 1888. Sci. Rep. Tohoku Univ., Ser. *VII*, 37, 159-173.
Yoshinaga, T. and Nakagawa, M. (1999) Finding of primary basalt from Sannome-gata volcano, northeastern Japan, and its compositional

variation. Jour. Min. Pet. Econ. Geol., **94**, 241-253. (in Japanese with English abstract)